Paläontol Z (2014) 88:329–352
DOI 10.1007/s12542-013-0200-6

RESEARCH PAPER

Study of a digital cranial endocast of the non-mammaliaform cynodont *Brasilitherium riograndensis* (Later Triassic, Brazil) and its relevance to the evolution of the mammalian brain

Pablo Gusmão Rodrigues · Irina Ruf · Cesar Leandro Schultz

Received: 19 March 2013 / Accepted: 2 August 2013 / Published online: 25 August 2013

Abstract A digital cranial endocast of the specimen UFRGS-PV-1043-T, *Brasilitherium riograndensis*, was obtained from high-resolution computed tomography (μCT) scan images. This taxon is a small cynodont from the Late Triassic of Brazil, and has been used as the sister-group of the mammaliaforms in cladistic analyses. The digital endocast of UFRGS-PV-1043-T is mostly complete, allowing the description and collection of accurate linear and volumetric measurements, which were taken and compared with other non-mammaliaform cynodonts. Impressions of vessels were observed in the inner walls of the braincase. Despite the lack of a cribiform plate and the presence of a wide orbital vacuity, the endocast of *Brasilitherium* shows olfactory bulb casts that are relatively larger than in other non-mammaliaform cynodonts, suggesting a pattern of gradual increase in size and improvement of the olfactory sense for these structures toward the mammalian condition. The cerebral hemispheres are elongated and clearly divided by a median sulcus. The parafloccular casts are well defined, and their position corresponds to the maximum width of the endocast. In the ventral view, a large hypophyseal cast and a wide opening for the cavum epiptericum are evident. The encephalization quotient (EQ) calculated for *Brasilitherium* is greater than the range of EQs reported for most non-mammaliaform cynodonts (although it may be similar to that of some taxa, according to the equation used to estimate their body masses), but it is smaller than that of the mammaliaforms and mammals. A slighter increase in the brain size of *Brasilitherium* compared with other non-mammaliaform cynodonts was observed, along with a more significant increase in the size of the olfactory bulbs. This study supports the proposition of an early evolution of the mammalian brain associated with selective pressures for better sensorial acuity, especially regarding improved olfaction, which began with small Triassic mammaliamorphs.

Keywords Mammalian brain evolution · Endocast · *Brasilitherium* · Cynodonts · μCT scan · Triassic

Kurzfassung Mittels μCT-Daten wurde ein virtueller Gehirnausguss von *Brasilitherium riograndensis* (UFRGS-PV-1043-T) erstellt. Bei diesem Taxon handelt es sich um einen kleinen Cynodontier aus der späten Trias von Brasilien, der in cladistischen Analysen die Schwestergruppe der Mammaliaformes repräsentiert. Der fast vollständige virtuelle Gehirnausguss von UFRGS-PV-1043-T ermöglicht die Beschreibung sowie genaueste lineare und volumetrische Messungen im Vergleich mit anderen nicht-mammaliaformen Cynodontier. Am inneren Schädeldach befinden sich einige Abdrücke von Blutgefässen. Obwohl eine Lamina cribrosa fehlt und die Augenhöhlen sehr groß sind, weist der virtuelle Ausguss von *Brasilitherium* relativ größere Bulbi olfactorii auf als bei anderen nicht-mammaliaformen Cynodontiern. Somit lässt sich eine graduelle Größenzunahme sowie Verbesserung des Riechsinns hin zu

P. G. Rodrigues (✉) · C. L. Schultz
Laboratório de Paleovertebrados, Departamento de Paleontologia e Estratigrafia, Instituto de Geociências, Universidade Federal do Rio Grande do Sul, Avenida Bento Gonçalves, Porto Alegre, RS 9500, Brazil
e-mail: pablogr@bol.com.br

C. L. Schultz
e-mail: cesar.schultz@ufrgs.br

I. Ruf
Steinmann-Institut für Geologie, Mineralogie und Paläontologie, Rheinische Friedrich-Wilhelms-Universität Bonn, Nussallee 8, 53115 Bonn, Germany
e-mail: irina.ruf@uni-bonn.de

einem säugerähnlichen Zustand beobachten. Die Großhirnhälften sind verlängert und deutlich durch einen medianen Sulcus voneinander getrennt. Die Paraflocculusausgüsse sind deutlich ausgeprägt und ihre Lage korrespondiert mit der maximalen Breite des gesamten Gehirnausgusses. In ventraler Ansicht ist ein prominenter Ausguss der Hypophyse sowie eine große Öffnung in das Cavum epiptericum zu erkennen. Der für *Brasilitherium* berechnete Enzephalisationsquotient (EQ) ist größer als die Spannbreite der EQs der meisten anderen nicht-mammaliaformen Cynodontier. Aufgrund der Schätzung des Körpergewichts von *Brasilitherium* könnte dessen EQ jedoch dem bestimmter Taxa durchaus entsprechen; er ist jedoch sicherlich geringer als bei Mammaliaformes und Mammalia. *Brasilitherium* zeigt eine geringere Größenzunahme des Gehirns im Vergleich zu anderen nicht-mammaliaformen Cynodontiern, mit wesentlich deutlicherer Größenzunahme der Bulbi olfactorii. Diese Studie unterstützt die Annahme einer frühen Evolution des Säugergehirns assoziiert mit der Selektion erhöhter sensorischer Schärfe, insbesondere der Verbesserung der Riechleistung, die bereits bei triassischen kleinen Mammaliamorpha auftritt.

Schlüsselwörter Evolution des Säugergehirns · Neuroanatomie · *Brasilitherium* · Cynodontier · μCT · Trias

Introduction

Living mammals are distinguished by relatively larger and more complex brains than other vertebrates (Kielan-Jaworowska et al. 2004; Kemp 2009). These large, complex brains can be considered the most biologically significant characteristic of mammals, because this enhanced central neural capacity is, directly or indirectly, associated with many aspects of the mammalian physiology and behavior (Kemp 2009). Study of the evolution of such a brain, involving increasing sensory acuity and motor control adaptations for locomotion, is therefore essential to understanding the origin of mammals (Jerison 1973; Ulinski 1986; Rowe et al. 2011).

The greater capacity of the mammalian brain in relation to other vertebrates is generally attributed to the development of the neocortex (Kielan-Jaworowska et al. 2004), or isocortex, a six-layer portion of the dorsal pallium (or neopallium) that receives sensory projections from other portions of the brain (Butler and Hodos 1996; Nieuwenhuys et al. 1998). Ulinski (1986) also mentions the striatum, involved in motor coordination, as a leading region in the evolution of the mammalian telencephalon. With the integration of sensory information and the coordination of motor responses in the brain, paleoneurological studies help us understand the behavior of extinct animals, as well as the evolution of their sensory systems and their relationship to other anatomical and biomechanical changes (Rowe et al. 2011).

Knowledge about the evolution of the mammalian brain is dependent on the study of the brains of the non-mammalian cynodonts. Because the preservation of soft tissues in fossils is extremely rare, paleontologists rely heavily on cranial endocasts to study the brain and central nervous system in extinct animals (e.g., Edinger 1948, 1955; Radinsky 1981; Quiroga 1984; Macrini et al. 2007a, b). It is noteworthy that cranial endocasts do not provide any direct information about the internal structure of the brain, such as the morphology of the neurons, number of neurons, neuron density, or neuron connectivity (Deacon 1990). In addition, the intracranial space is not occupied solely by the brain; there are other soft tissue structures, such as the meninges, blood vessels, and nerves.

Nevertheless, some neuroanatomical external features can be identified from endocasts of some taxa. This is especially the case for mammals and birds, because their brains largely fill the endocranial space, leaving impressions on the internal surfaces of the skull bones (Jerison 1973). In the small-brained non-mammalian and non-avian tetrapods, the brain does not fully occupy the endocranial cavity (Starck 1979). Indeed, cranial endocast studies only provide an approximation of the external features of the brain; nevertheless, they can provide important neuroanatomical information, and the differences found between taxa can be associated with the phylogeny in an evolutionary approach.

Thus, the evolution of the mammalian brain has long been studied using fossil endocasts (e.g., Simpson 1927, 1937; Edinger 1942, 1948, 1955, 1964; Radinsky 1968a, b, 1973a, b, 1976, 1977; Jerison 1973, 1991; Kielan-Jaworowska 1983, 1984, 1986; Rowe 1996). For non-mammaliaform cynodonts, endocast descriptions have been published initially for the Early Triassic taxa *Nythosaurus larvatus* (possibly *Thrinaxodon liorhinus*) and *Diademodon* by Watson (1913). Later, endocasts of the Late Triassic *Exaeretodon* (Bonaparte 1966), the Early Triassic *Trirachodon* (Hopson 1979), the Late Permian *Procynosuchus* (Kemp 1979), the Middle Triassic *Massetognathus* and *Probelesodon* (Quiroga 1979, 1980a), *Probainognathus* (Quiroga 1980b, c) and the Late Triassic *Therioherpeton* (Quiroga 1984) were described.

In general, these works (except Kemp 1979) delineate for these non-mammaliaform cynodonts the same basic design, suggesting narrow brains with tubular cerebral hemispheres. However, Kemp (2009) suggested that in non-mammaliaform cynodonts, the region of the cerebral hemispheres could have been substantially deeper than

wide, because there is no brain cavity floor in that region of the skull. A bony floor formed by the orbitosphenoid is reported for some non-mammaliaform cynodonts such as *Trirachodon*, *Massetognathus* and *Probelesodon*, but a lateral bony closure for the most anterior region of the brain is only observed in tritylodontids (e.g., Kielan-Jaworowska et al. 2004). The olfactory bulbs and the cerebellar region, with prominent paraflocculi, are other visible structures described in the endocasts of the above-cited non-mammaliaform cynodonts. However, the vermis of the cerebellum was not reported in these descriptions (Watson 1913; Hopson 1979; Quiroga 1979, 1980a, b, 1984), although its presence is indicated by Kielan-Jaworowska et al. (2004) for the eucynodont *Thrinaxodon*.

The first clear change observed from the endocasts of the non-mammaliaform cynodonts is the loss of the parietal eye (and perhaps the whole parietal-pineal complex) in most Eucynodontia taxa, although some eucynodonts, such as *Diademodon, Trirachodon* and *Massetognathus*, present the primitive state (e.g., Hopson and Kitching 2001). The division between the cerebral hemispheres seems to be more defined in *Probainognathus* (Quiroga 1980a, b) than in *Thrinaxodon* (Kielan-Jaworowska et al. 2004), *Exaeretodon* (Bonaparte 1966), *Massetognathus* and *Probeleson* (Quiroga 1979). Indeed, Quiroga (1980a, b) suggested the presence of a neocortex (isocortex) in the *Probainognathus* endocast, but the sulcus, interpreted by him as the posterior limit of this region, was later considered a blood vessel mark at the external surface of the brain (Kielan-Jaworowska 1986). Due to the presence of the clearest division of the cerebral hemispheres and by a slight lateral expansion at the posterior region of these structures, *Probainognathus* presents the most derived condition among the non-mammaliaform cynodonts with endocasts described to date.

Among non-mammalian mammaliaforms, Luo et al. (2001) reported a progressive enlargement of the posterior (cerebellar) region in *Sinoconodon*, *Haldanodon*, *Morganucodon*, and *Hadrocodium*. Moreover, an enlargement of the cerebral hemisphere region of *Morganucodon* and *Hadrocodium* is represented in the summarization of Kielan-Jaworowska et al. (2004). In the endocast of *Morganucodon*, the authors highlighted the presence of a lateral divergence between the cerebral hemispheres posteriorly and the presence of marks interpreted as transversal gyres at the dorsal surface of the cerebellum cast. Moreover, the cerebral hemisphere region is relatively wider in *Morganucon* compared with the non-mammaliaform cynodonts and *Sinoconodon*, in which the parietal bones are subvertically disposed, therefore having less endocranial space in this region (Kielan-Jaworowska et al. 2004). Another feature suggested to be derived in *Morganucodon* (Kermack et al. 1981) is the division of the cerebral and cerebellar cavities by an ossified septum, i.e., the tentorium (tentorium osseum), but this suggestion is controversial (e.g., Kielan-Jaworowska 1997).

Considering the significant relative increase observed in the brain of *Morganucodon* (in relation to non-mammaliaform cynodonts) and *Hadrocodium* (in comparison with other non-mammalian mammaliaforms), Rowe et al. (2011) indicated that these two taxa mark two "pulses" of encephalization, most likely involving the development of the neocortex in these taxa, inferred by the enlargement of the hemispheres. Despite the absence of an impression of the rhinal fissure on the endocasts, Rowe et al. (2011) also based their inference about the presence of a neocortex in *Morganucodon* (in relation to non-mammaliaform cynodonts) and *Hadrocodium* on the presence of a thick coat in another non-mammalian, *Castorocauda lutrasimilis* (Ji et al. 2006). Rowe et al. (2011) used this evidence as indicative of a neocortex, because it is initially predominant in this region of the brain, an area that controls the somatosensory mechanoreceptors of skin and hair follicles, as well as proprioceptors (muscle spindles) and joint receptors.

The olfactory bulbs in *Triconodon* and multituberculates are more spherical, and the cerebellum expands laterally (Kielan-Jaworowska et al. 2004). The presence of a hypertrophied vermis cerebelli was initially suggested (Simpson 1937; Jerison 1973; Kielan-Jaworowska 1986, 1997) for these taxa, but Kielan-Jaworowska and Lancaster (2004) interpreted the same region as corresponding to a large blood vessel, the superior cistern, which would preclude visualization of the true vermis cerebelli and part of the midbrain. Thus, the general appearance of the brain of these animals would be similar to that of the first Theria. For the Mammalia crown group, Kielan-Jaworowska et al. (2004) mentioned another enlargement of the cerebral hemispheres and the cerebellum, especially between the vermis and the parafloccculus, associated with an enlargement of the braincase at the region above the fossa subarcuata and above the lambdoidal crest. The exposure of the dorsal part of the midbrain as observed in didelphids, *Leptictis*, *Labidolemur*, *Tenrec* and *Rhynchocyon* most likely represents the primitive condition for the early placentals (Bauchot and Stephan 1966, 1967; Novacek 1986; Kielan-Jaworowska et al. 2004; Silcox et al. 2011). Among living mammals, however, the midbrain is fully covered by the cerebral hemispheres in monotremes and eutherians (e.g., Macrini et al. 2007b). The identification of vascular channels of the transverse sinus, which mark the posterior limit of the cerebral hemispheres, in Later Cretaceous placentals is taken by Kielan-Jaworowska et al. (2004) as evidence that the exposure of the midbrain area in the endocast of those animals actually corresponds to that portion of the brain. For older taxa, in which a clear

definition of the transverse sinus does not exist, the same authors warn about the possibility that the "midbrain region" exposed in the endocast resulted in post-mortem changes to parts of the brain and meninges.

In addition to the anatomical features observed in the endocasts, a quantitative approach provided by the Encephalization Quotient (EQ) has been widely utilized, and criticized (e.g., Deacon 1990; Striedter 2005). The EQ, as developed by Jerison (1973) and discussed by Eisenberg (1981), represents the expected brain weight (for a fossil taxon) in relation to the body weight using the same ratio (brain weight/body weight) obtained from a taxonomic group of reference. An initial criticism of this approach concerns the significance of the relative brain mass as an indicator of the capacity to integrate information from the environment by the different sensorial systems or some other definition of "intelligence". Moreover, the selective pressures for body and brain size can be independent (aquatic animals, for example, can achieve larger body masses due the buoyant environment), which can weaken the significance of this allometric relationship (Butler and Hodos 1996). Regarding methodological issues, it must be mentioned that the equations used to derive EQs vary depending on the data included in the study. For example, the exponent for a general sampling across Mammalia varies between 0.67 and 0.76. Eisenberg and Wilson (1978, 1981) and Eisenberg (1981) determined exponents of approximately 0.74 or 0.75, but the EQs reported for non-mammalian cynodonts by Jerison (1973) and Quiroga (1979, 1980a, b) were obtained using a mammalian exponent of 0.67. Moreover, for extinct taxa there are methodological difficulties to finding the actual weights for the brain and body, because the body mass must be estimated from different parameters in the fossils (skull length, skull width, postcanine teeth, lengths of long bones, mid-shaft circumferences of long bones, cross-sectional area of vertebrae), and the endocast volume (assuming that 1 cm^3 is equivalent to 1 g) cannot correspond to the actual volume occupied by the brain in the endocranial cavity.

Higher EQ values for different mammal taxa seem to be correlated with ecological variables, such as foraging behavior and social interactions (Eisenberg and Wilson 1978, 1981; Dunbar 1995; Striedter 2005). Studies utilizing the EQ for non-mammalian cynodonts indicate an increased brain volume in relation to the estimated body mass in taxa successively more closely related to mammals. An example is the EQs of the non-mammalian mammaliaforms *Morganucodon* (0.32) and *Hacrocodium* (0.49) reported by Rowe et al. (2011) compared with the EQs reported by Jerison (1973) and Quiroga (1979, 1980a, b) for non-mammaliaform cynodonts, with values ranging from 0.1 to 0.22.

The transition from non-mammaliaform cynodonts to mammaliaforms can help elucidate the major steps in the evolution of the mammalian brain. A crucial taxon of this evolutionary transformation is a mammaliamorph cynodont from the Late Triassic of southern Brazil, *Brasilitherium riograndensis* Bonaparte et al. 2003. This cynodont is considered the sister-group of Mammaliaformes, which are closer to mammals than the tritylodontids and tritheledontids (Bonaparte et al. 2003, 2005; Abdala 2007, Liu and Olsen 2010; Fig. 1). This taxon was recently considered a junior synonym of *Brasilodon quadrangularis*, which is found in the same outcrops, by Liu and Olsen (2010). They argue that the two taxa are not distinguishable based on the five characters used by Bonaparte et al. (2005), mainly due to incomplete and fragmentary data from the available samples. Notwithstanding, *Brasilodon* and *Brasilitherium* do not appear as sister groups in all phylogenetic analyses (e.g., Abdala 2007), and more studies and/or more samples are needed to solve this controversy. For now, because the sample used in this study was described as *Brasilitherium*, we have chosen to use the name originally proposed. This usage does not change the features of the specimen herein described and the sister-clade status of Brasilodontidae to Mammaliaformes, whatever the species status of *B. riograndensis* within the brasilodontid family. Therefore, the question of the purported synonymy will not affect the objective of the current paper.

Here, we present the first description of a digitally reconstructed cranial endocast of *B. riograndensis* based on high-resolution computed tomography (μCT) of the specimen UFRGS-PV-1043-T. The characters observed in this specimen are compared with other non-mammalian cynodonts to discuss the evolution of the mammalian brain.

Materials and methods

The specimen UFRGS-PV-1043-T

The specimen (Fig. 2) belongs to the collections of the Laboratório de Paleontologia de Vertebrados of the Universidade Federal do Rio Grande do Sul (UFRGS) in Porto Alegre, Rio Grande do Sul state, Brazil. This specimen was collected from the Upper Triassic Caturrita Formation (Late Carnian/Early Norian), corresponding to the upper levels of the Santa Maria 2 Sequence (Zerfass et al. 2003) in the outcrop Linha São Luiz (29°33′28.8″S; 53°26′53.6″W; Datum: Córrego Alegre) near the town of Faxinal do Soturno, Rio Grande do Sul state, Brazil.

UFRGS-PV-1043-T consists of a virtually complete skull without the lower jaw. Although the skull is well preserved, some bones are broken and distorted due to post-morten deformations: (1) there is an inclination of the braincase to the right; (2) the quadrate ramus of the pterygoid and epipterygoid (alisphenoid) is absent in the right

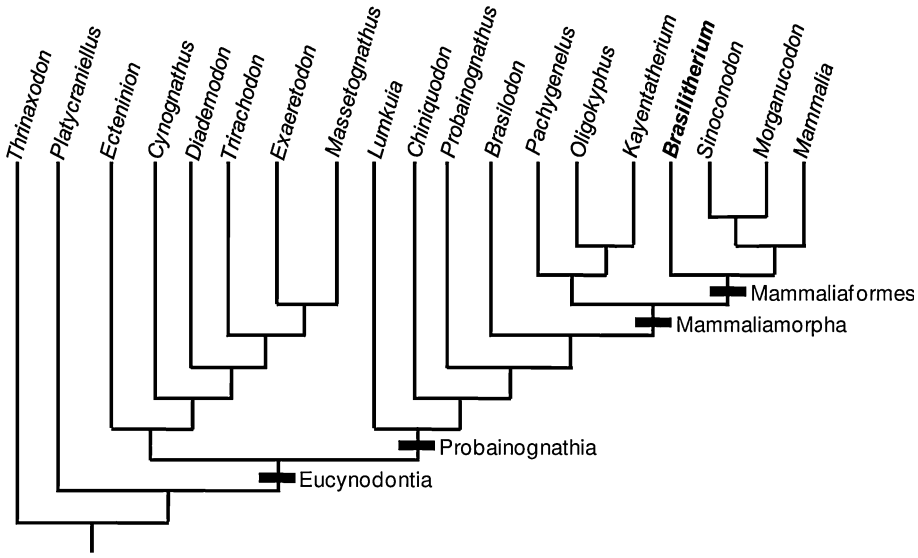

Fig. 1 Cladogram showing the phylogenetic relationships among the better-known cynodont taxa (including Mammalia) according to the analysis of Abdala (2007). The condition of *Brasilitherium* as the sister-group of the mammaliaforms is highlighted

side, which resulted in an incomplete filling of the cavum epiptericum at this side (see Fig. 5); (3) there is a linear fracture behind the frontal bones that can be seen in dorsal and lateral views and that crosses the entire skull vertically (Fig. 2a, b); (4) there is a broken bone (most likely the supraoccipital) in the most posterior region of the skull. Notwithstanding, these damages did not cause significant distortions in the overall endocast.

μCT scanning and digital extraction of the endocast

The sample was scanned using the Wälischmiller RayScan 200 μCT scanner located at Steinbeis-Transferzentrum Gießerei Technologie Aalen, Fachhochschule Aalen, Germany. A total of 884 slices (Fig. 3) were generated in coronal planes, with a resolution of 1,024 × 1,024 pixels and a voxel size of 0.0464 × 0.04634 × 0.04634 mm. The visualization of the slices, 3D rendering, measurements, segmentation and treatment of the images to separate the rocky matrix from the bony elements were performed using the software VGStudio Max© (version 1.2.1; Volume Graphics GmbH, 2004). The brain endocast and the inner ear endocast (whose description is presented in a separate paper; Rodrigues et al. 2013) were reconstructed using the infilling material in the cranial cavity and the bony labyrinth region of the skull, respectively. The slices were also manually treated to obtain a perfect distinction between bone tissue and the filling of the skull's internal cavities. Measurements of the brain endocast are presented in Table 1.

Due to the absence of an ossified floor for the most anterior region of the brain in *Brasilitherium*, we chose to digitally remove part of the filling of the orbital vacuity to better define the ventral contour of the olfactory bulb casts, because the rock matrix that forms the endocast in this region of the skull reaches the pterygoids. To estimate the ventral morphology of the olfactory bulbs, we relied on the casts clearly observable at the ventral surface of the frontals that delimitate two bulbs that are anteroposteriorly and laterally convex, separated by a median sulcus. Thus, based on this dorsal morphology, we set the ventral contour from the observation of the olfactory bulb casts in lateral view, assuming that the bulbs were dorsoventrally symmetrical (see Fig. 5), while taking into account that in endocasts described in the literature (e.g., Quiroga 1979, 1980a, b, c, 1984; Macrini et al. 2006, 2007a, b; Rowe et al. 2011), the olfactory bulbs usually have a ventral contour similar to the dorsal contour in lateral. Consequently, the volume of the olfactory bulb casts as well as the volume of the whole endocast is estimated from this digital reconstruction of the ventral portion of the olfactory bulb region.

Quantitative analysis

To calculate the EQ for *B. riograndensis*, it was necessary to estimate its body mass first. Because we do not have postcranial bones associated with any of the known skulls for this taxon, the body mass was estimated from the skull length using the equation utilized by Luo et al. (2001) for the Jurassic mammaliaforms *Sinoconodon*, *Morganucodon* and *Hadrocodium* (based on the scaling relationship of body mass to skull size in 64 species of living lipotyphlan insectivore mammals presented by Gingerich and Smith 1984). The regression equation is $X = 3.68Y - 3.83$, where X is the $\log_{10}$ of the body mass in grams and Y is the logarithm of the skull length in millimeters.

The EQ was calculated from the endocast volume (EV) and the estimated body mass (BM), which was obtained using two different equations: $EQ = EV/0.12BM^{0.67}$, from Jerison (1973), and $EQ = EV/0.055BM^{0.74}$, from Eisenberg (1981), as presented in Table 2.

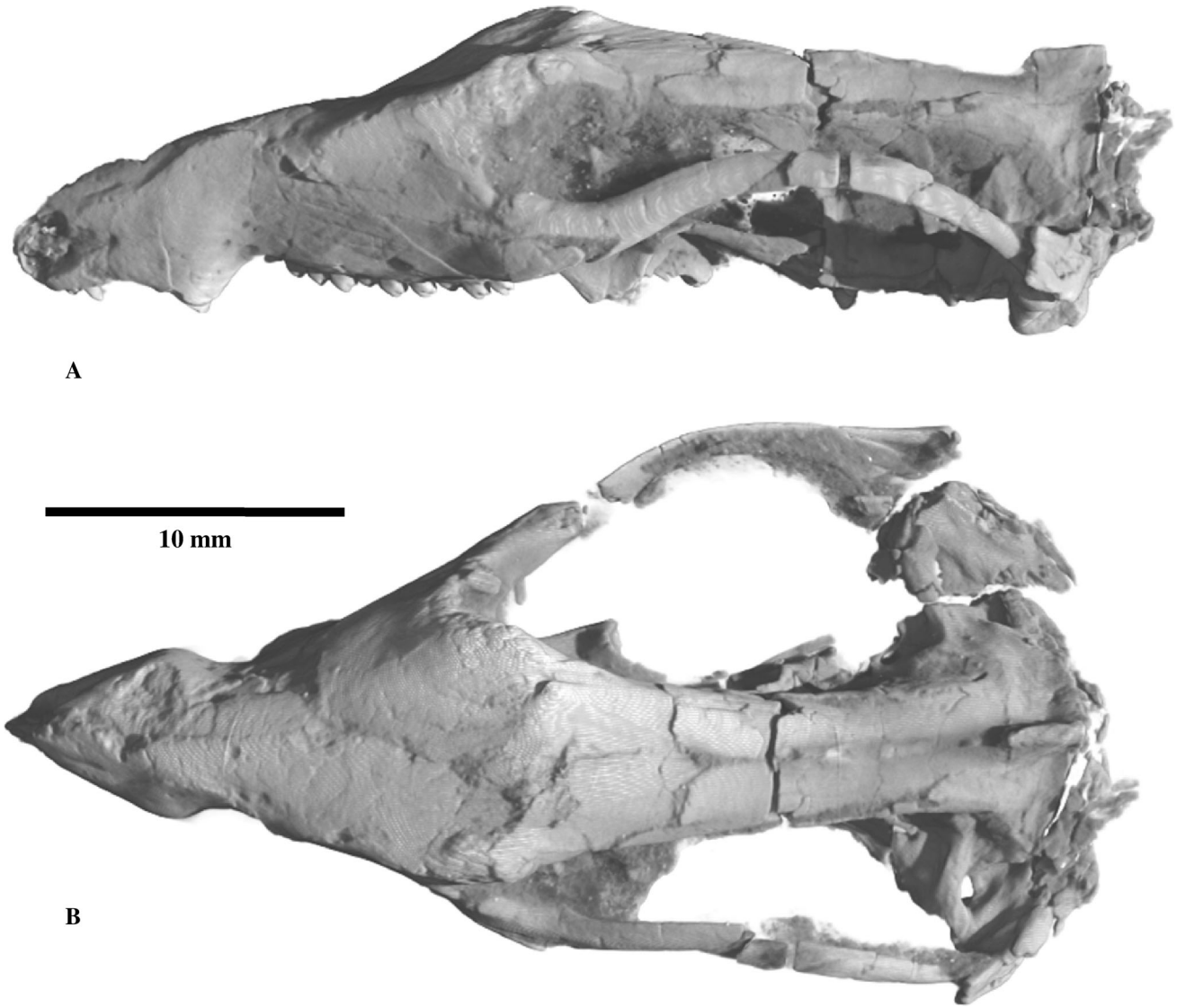

Fig. 2 Digital three-dimensional (3D) reconstruction of skull UFRGS-PV-1043-T obtained from the μCT scan images. **a** Left lateral view. **b** Dorsal view

Description and comparisons

General aspects

The endocranial cast of *Brasilitherium* UFRGS-PV-1043-T in dorsal view (Fig. 4) shows two anterior oval structures that correspond to the olfactory bulbs, followed by two longer structures, apparently cylindrical, but gradually wider posteriorly, corresponding to the cerebral hemispheres. There is a small posterior area, narrower than the widest portion of the cerebral hemispheres, that corresponds to the dorsal surface of the cerebellum. The total length of the endocranial cast (Table 1), from the anterior limit of the dorsal surface of the olfactory bulbs to the foramen magnum, is 17.67 mm, corresponding to 46.5 % of the total length of the skull (38.03 mm). The maximum width is 7.17 mm, taken at the point where two laterally bulging structures are placed, located below the dorsal surface of the cerebral hemispheres approximately 1 mm from the foramen magnum. These structures fill the fossa subarcuata on both sides and correspond to the cerebellar paraflocculi. The endocranial cast is elongated, with a width to length ratio of approximately 0.4.

The lateral profile (Fig. 5) of the endocranial cast of the specimen UFRGS-PV-1043-T reveals an anteroposteriorly

Fig. 3 Digital 3D reconstruction of skull UFRGS-PV-1043-T in dorsal view (*above*), with *lines* (*A*, *B*, *C*, and *D*) indicating the positions of four slices (556, 653, 706 and 743), which are shown in images **a**–**d** (*below*), respectively. Cranial bones and other anatomical features interpreted from the slices are indicated ▶

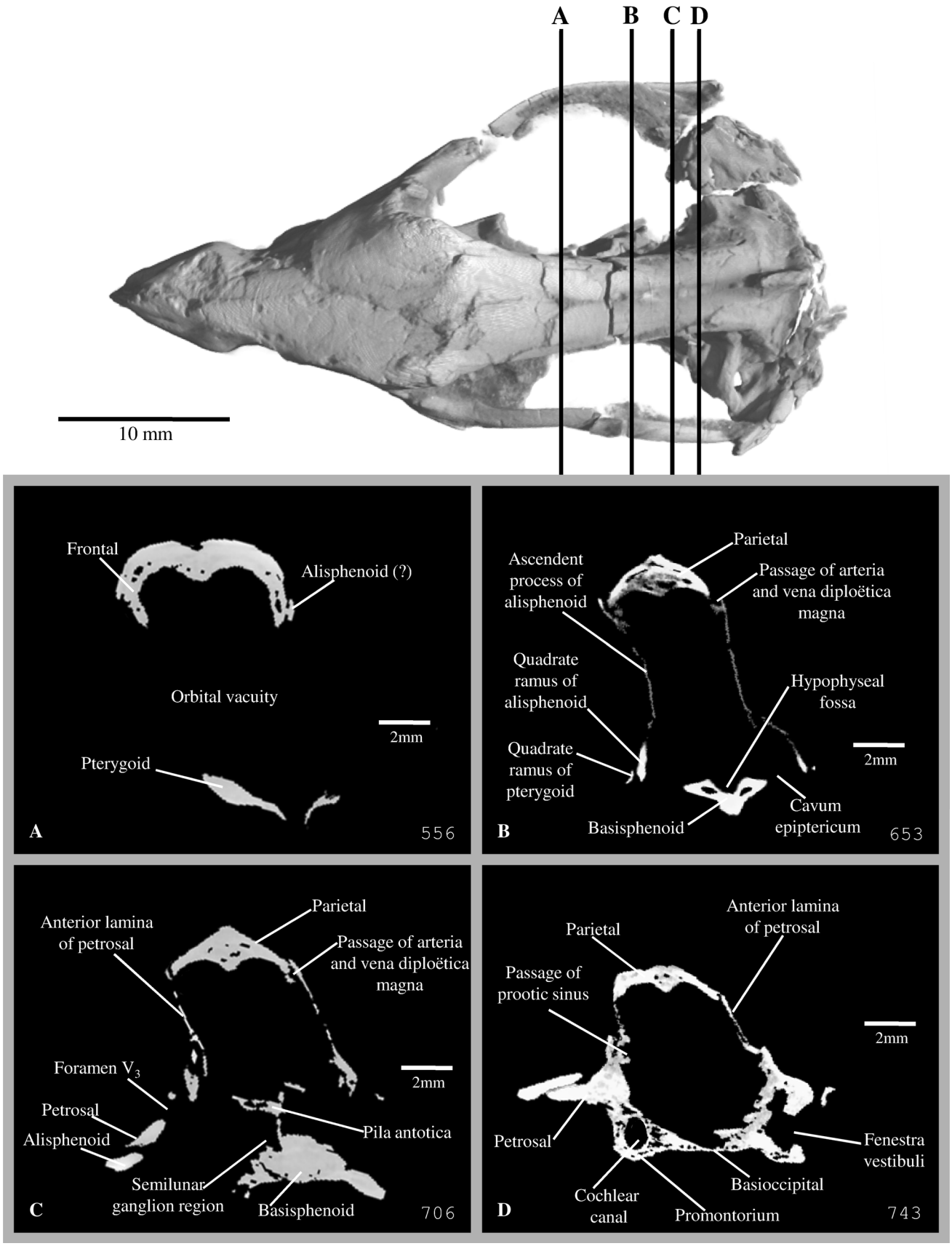
A
B
C
D
10 mm
Frontal
Alisphenoid (?)
Orbital vacuity
2mm
Pterygoid
A
556
Parietal
Ascendent process of alisphenoid
Passage of arteria and vena diploëtica magna
Quadrate ramus of alisphenoid
Hypophyseal fossa
2mm
Quadrate ramus of pterygoid
Basisphenoid
Cavum epiptericum
B
653
Anterior lamina of petrosal
Parietal
Passage of arteria and vena diploëtica magna
Foramen V3
2mm
Petrosal
Alisphenoid
Pila antotica
Semilunar ganglion region
Basisphenoid
C
706
Anterior lamina of petrosal
Parietal
Passage of prootic sinus
2mm
Petrosal
Fenestra vestibuli
Basioccipital
Cochlear canal
Promontorium
D
743

Table 1 Measurements of the digital brain endocast of UFRGS-PV-1043-T, *Brasilitherium riograndensis*

Length, measured from the anterior limit of the dorsal surface of the olfactory bulb to the foramen magnum (the length of the endocast as shown in Figs. 4 and 5a)	17.67 mm
Length, measured from the estimated anterior limit of the olfactory bulbs to the foramen magnum* (the length of the endocast shown in Fig. 5b)	18.84 mm
Maximum width (between the paraflocculars casts)	7.17 mm
Maximum height, measured from the ventral limit of the hypophyseal cast to the dorsal surface above it	7.79 mm
Maximum height, corresponding to the distance between the ventral limit of the hypophyseal cast and the most dorsal point of the olfactory bulb casts)	8.31 mm
Volume of the endocast*	378.436 mm^3
Length of the dorsal surface of the two olfactory bulb casts (as shown in Figs. 4 and 5a)	6.10 mm
Length estimated for the olfactory bulb region* (see Fig. 5b)	9.04 mm
Maximum width of the olfactory bulb casts together	44.62 mm
Maximum width of the right olfactory bulb cast	2.36 mm
Maximum width of the right olfactory bulb cast	2.26 mm
Estimated volume for the region of the olfactory bulb region* (see Fig. 5b)	135.531 mm^3
Width at the point of the endocast immediately posterior to the dorsal bulging of the olfactory bulb casts	3.39 mm
Length of the dorsal surface of the region of the cerebral hemisphere casts	9.23 mm
Maximum width of the dorsal surface at the region of the cerebral hemisphere casts (above the dorsal vascular impressions)	5.21 mm
Maximum width of the region of the cerebral hemisphere casts below the dorsal vascular impressions	5.80 mm
Width of the anterior limit of the region of the cerebral hemisphere casts	3.60 mm
Width of the posterior limit of the region of the cerebral hemisphere casts	4.61 mm
Anteroposterior length of the dorsal surface of the cerebellar region	1.30 mm
Width of the dorsal surface of the cerebellar region	4.21 mm
Distance between the apex of the right paraflocular cast and the adjacent lateral surface (the axis of the paraflocular cast is lateroposteriorly inclined)	1.50 mm
Distance between the lateral limit of the right paraflocular cast and the adjacent lateral surface (the lateral limit is not the apex because the axis of the paraflocular cast is lateroposteriorly inclined)	1.20 mm
Maximum diameter of the right paraflocular cast	1.51 mm
Distance between the apex of the left paraflocular cast and the adjacent lateral surface (the axis of the paraflocular cast is lateroposteriorly inclined)	1.51 mm
Distance between the lateral limit of the left paraflocular cast and the adjacent lateral surface (the lateral limit is not the apex because the axis of the paraflocular cast is lateroposteriorly inclined)	1.32 mm
Maximum diameter of the left paraflocular cast	1.78 mm
Volume of the two paraflocular casts together	7.896 mm^3
Anteroposterior diameter of the hypophyseal cast	1.39 mm
Maximum width of the hypophyseal cast	1.28 mm
Height (depth) of the hypophyseal cast in relation to the adjacent ventral surface	0.62 mm
Volume of the hypophyseal cast	0.839 mm^3
Length of the ventral opening of the cavum epiptericum (left side)	4.67 mm
Maximum width of the ventral opening of the cavum epiptericum (left side)	2.29 mm

* Values based on the ventral contour and anterior limit estimated for the olfactory bulbs by removing part of the infilling of the orbital vacuity to make the ventral contour similar to the dorsal contour

Table 2 Endocast volume, estimated body mass and Encephalization Quotient (EQ) values calculated for *Brasilitherium* UFRGS-PV-1043-T

Endocast volume (EV)	Estimated body mass (*M*)	Encephalization quotient (EQ)	
		$EQ = EV/(0.12\ M^{0,66})$[a]	$EQ = EV/(0.055\ M^{0,75})$[b]
0.378436 ml	98.57 g	0.1482	0.2233

[a] Equation from Jerison (1973)

[b] Equation from Eisenberg (1981)

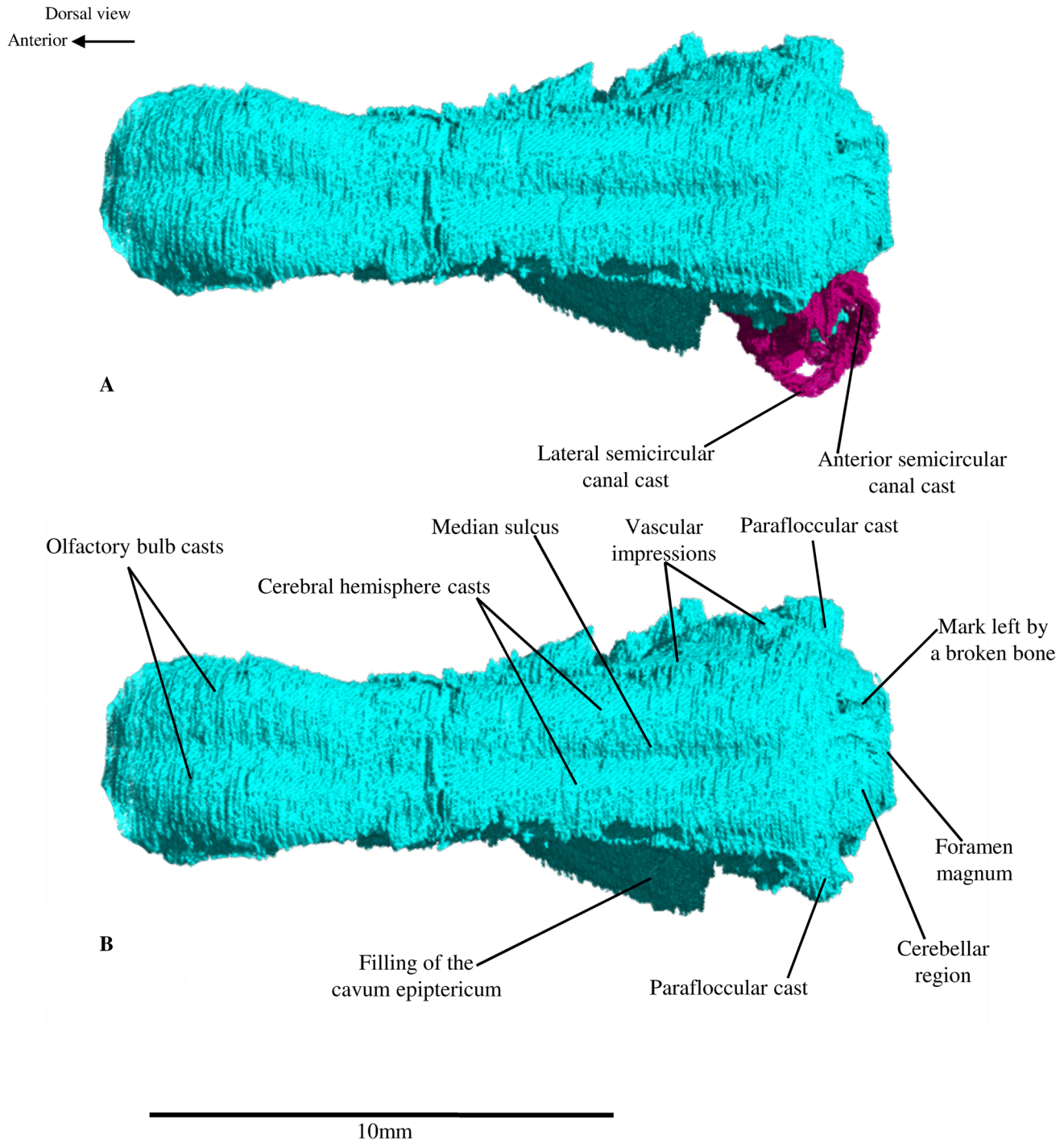

Fig. 4 Digital endocast of *Brasilitherium riograndensis* (UFRGS-PV-1043-T) in dorsal view. **a** Shows the inner ear cast (*purple*), which was digitally removed in **b**

convex dorsal surface on the olfactory bulbs. Behind this region, the dorsal contour becomes straight, with a slight slope in the posterior direction (approximately 4° relative to a hypothetical dorsal horizontal plane) along 8.5 mm. At that point, the slope becomes much steeper (42°) for approximately 1.6 mm, and the lowest point of this slope most likely marks the posterior limit of the brain hemispheres. Immediately behind that slope is a lower region corresponding to the dorsal surface of the cerebellum and associated meninges with an anteroposterior length of 1.3 mm, whose dorsal border presents a more gentle slope (28°) to the level of the foramen magnum.

The maximum height of the endocranial cast is 7.79 mm, measured as a vertical line from the ventral limit

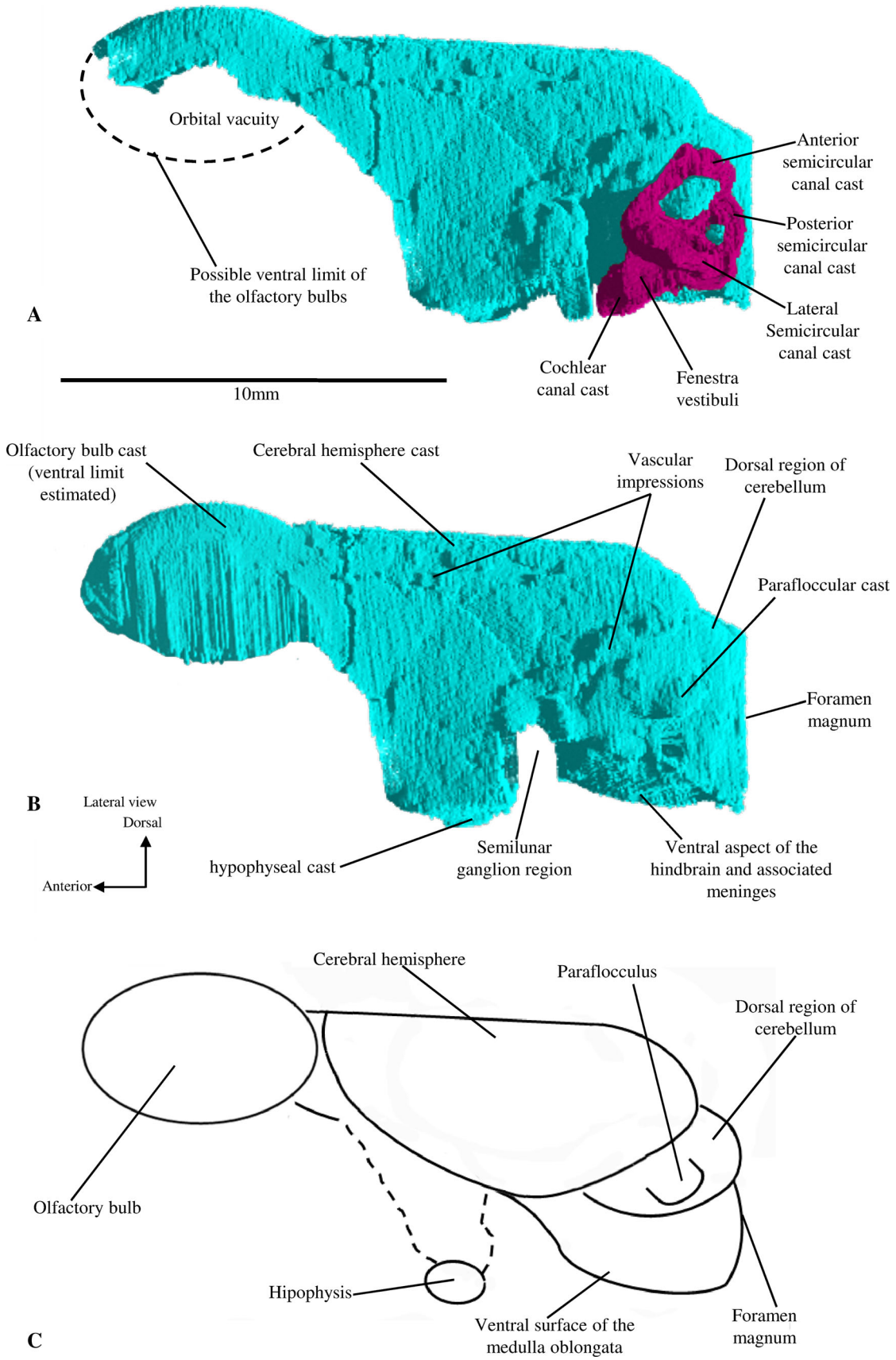
A
Orbital vacuity
Possible ventral limit of the olfactory bulbs
Anterior semicircular canal cast
Posterior semicircular canal cast
Lateral Semicircular canal cast
Cochlear canal cast
Fenestra vestibuli
10mm
B
Olfactory bulb cast (ventral limit estimated)
Cerebral hemisphere cast
Vascular impressions
Dorsal region of cerebellum
Parafloccular cast
Foramen magnum
Lateral view
Dorsal
Anterior
hypophyseal cast
Semilunar ganglion region
Ventral aspect of the hindbrain and associated meninges
C
Cerebral hemisphere
Paraflocculus
Dorsal region of cerebellum
Olfactory bulb
Hipophysis
Ventral surface of the medulla oblongata
Foramen magnum

◀ **Fig. 5** Digital endocast of *Brasilitherium* UFRGS-PV-1043-T in lateral view. **a** shows the left inner ear cast (*purple*). In **b**, the inner ear cast and the filling of the posterior half of the cava epipterica lateral to the pila antotica were digitally removed. **c** is a schematic illustration of the brain of *Brasilitherium* in lateral view, based on the endocast interpretation

of the hypophyseal fossa for the pituitary gland, with its dorsal limit at a point approximately half the length of the cerebral hemispheres. However, because the dorsal limit of the cast corresponds to the top of the olfactory bulbs, a maximum height of 8.31 mm can be considered as the vertical distance between the two horizontal lines corresponding to the dorsal and ventral limits of the endocranial cast. The ventral limit of the endocast, posterior to the orbital vacuity, is defined by the basicranial bones (basisphenoid/parasphenoid, basioccipital, petrosal). No neuroanatomical details are distinguishable in lateral view between the orbital vacuity and the paraflocculus cast, with the lateral wall of the endocast, at least in its ventral half, formed by the cavum epiptericum situated between the

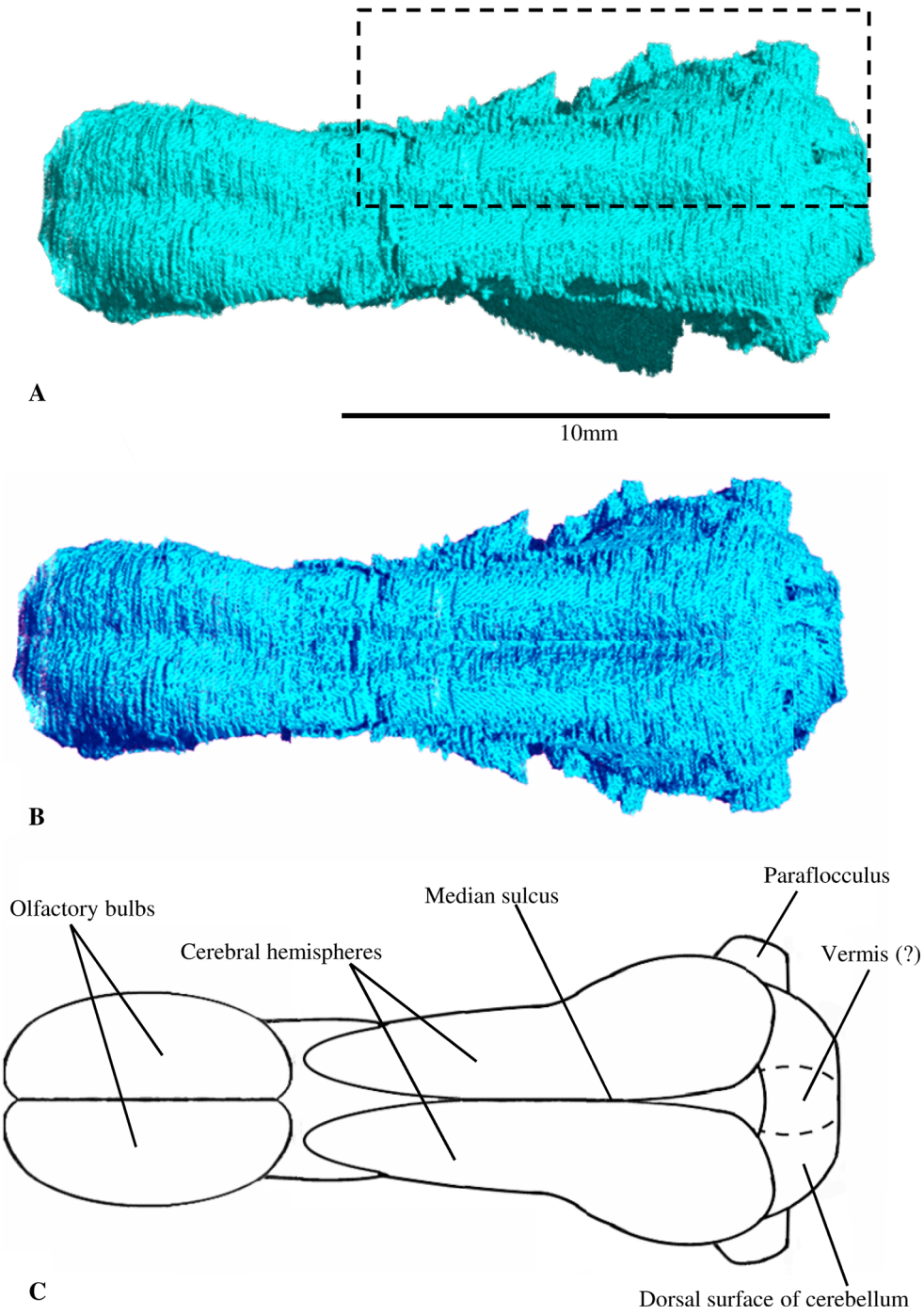

Fig. 6 Digital endocast of *Brasilitherium* UFRGS-PV-1043-T in dorsal view. **a** Highlights the part of the *right side* that was mirrored to the *left* (which is laterally compressed) in **b**, where both sides are presented symmetrically. **c** Shows a schematic representation of the interpretation of the dorsal view of the endocast without the deformation on the *left side*

ascending process of the alisphenoid and the pila antotica. Two impressions of blood vessels are visible in lateral view (Fig. 5) and dorsal view (Fig. 6), whose casts were isolated from the rest of the endocast (Fig. 7). One of these impressions corresponds to a line that runs along the suture between the parietal and the ascending process of the alisphenoid. The line then continues posteriorly, internal to the dorsal anterior lamina of the petrosal, curving posteroventrally toward the post-temporal canal. The other impression is diagonal, in posterodorsal direction, between the posterior region of the cavum epiptericum and a point above the paraflocculus cast. As indicated in Fig. 7, these vascular impressions must correspond to the ascending branch of the arteria and vena diploëtica magna and the sinus prooticus, respectively.

In Fig. 4, the endocast in lateral view is also shown with the filling of the posterior half of the cavum epiptericum (region of the semilunar ganglion of the trigeminal nerve

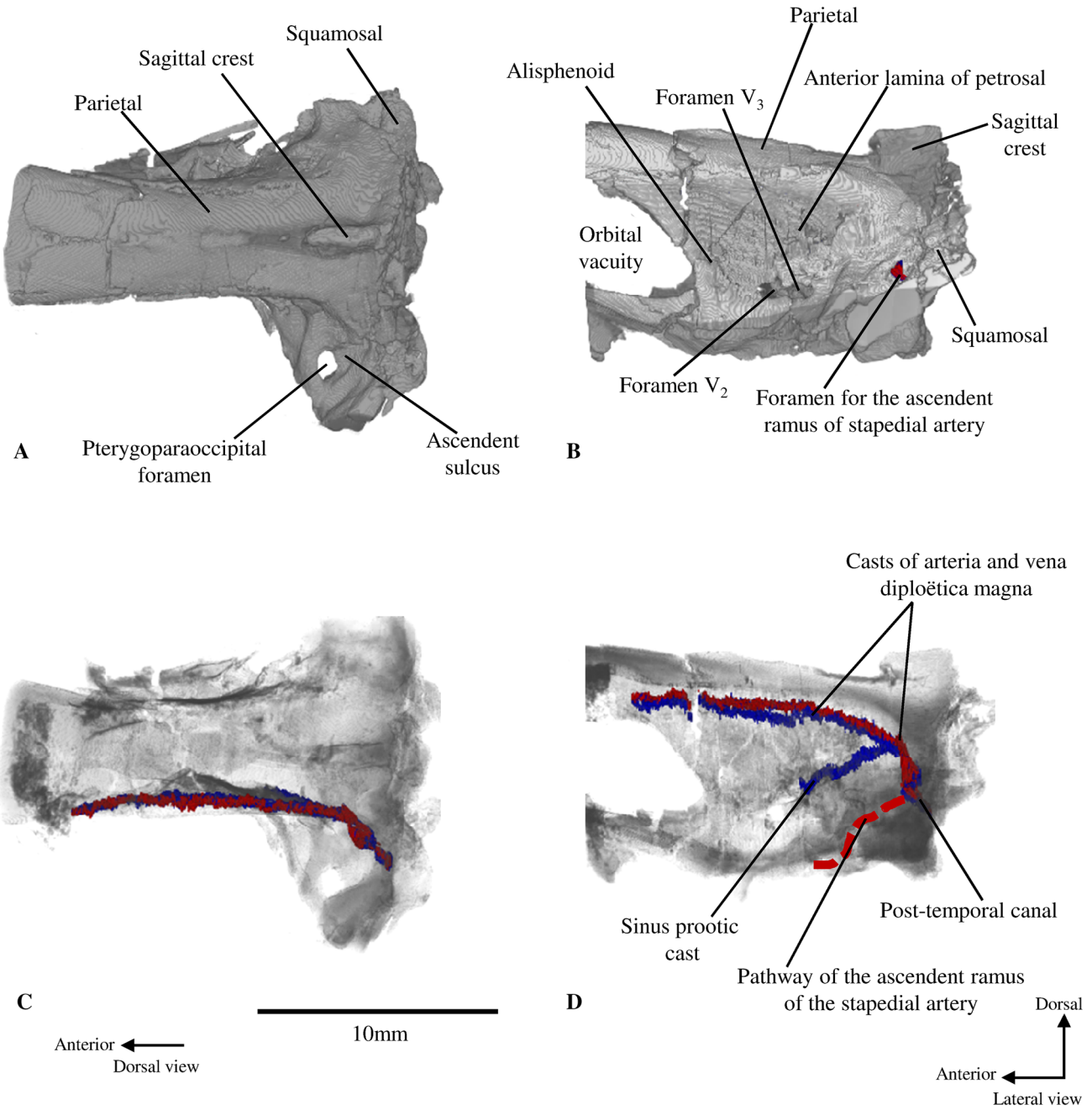

Fig. 7 Posterior half of the 3D reconstruction of the skull in dorsal (*left*: **a**, **c**) and lateral (*right*: **b**, **d**) view. Below (**c, d**), semi-transparence was applied to the bony elements to show the casts of veins (*blue*) and arteries (*red*). The *dashed line* schematically shows the external path of the stapedial artery

V) digitally removed, thus revealing the ventral surface of the endocranial cast from the region of the hindbrain and associated meninges to the foramen magnum, but without differentiating the medulla oblongata and pons. This region has a distinct anteroposterior convexity (approximately 4 mm in length), whose maximum ventral projection (approximately 0.3 mm below the horizontal line of the lower limit of the foramen magnum) corresponds to the limit of the ventral portion of the endocast posterior to the hypophyseal fossa. Anteriorly to that region and medial to the posterior half of the cavum epiptericum (which was digitally removed), the ventral surface of the endocast leans abruptly in the anterodorsal direction (63° to the horizontal line of the lower limit of the foramen magnum), suggesting that the ventral contour of these parts of the brain is placed approximately 2 mm above the ventral limit of the endocast posterior to the cavum epiptericum (Fig. 5). However, this portion is visible (removing the posterior half of the cavum epiptericum filling) only by a length of 1.8 mm in the anteroposterior direction. Anteriorly to this stretch, there is no way to identify the ventral contour of the endocast, except by the presence of the hypophyseal cast, which only constitutes the more ventral point of the endocast (approximately 0.4 mm below the horizontal line of the lower limit of the foramen magnum).

In ventral view (Fig. 8), the semi-spherical cast of the hypophyseal fossa (sella turcica) is a prominent structure located in the midline of the ventral surface, slightly behind the center of the endocranial cast in the anteroposterior direction. In this sense, the center of the hypophyseal fossa cast is placed approximately 10 mm from the anterior limit of the olfactory bulb casts and 7 mm from the posterior limit of the foramen magnum. The hypophyseal fossa cast of *Brasilitherium* is nearly circular, with a maximum width (1.28 mm) to anteroposterior length (1.39 mm) ratio of 0.92, corresponding to approximately 8 % of the total length of the endocast. The height or depth of the hypophyseal cast in relation to the adjacent ventral surface is 0.62 mm. The hypophyseal cast, then, is represented by a semi-sphere that fills the sella turcica, whose volume (0.84 mm^3) corresponds to 0.22 % of the estimated volume of the brain endocast (see the quantitative analysis below).

Although the hypophyseal cast can be considered a poor indicator of the size and/or shape of the pituitary gland (hypophysis) in many mammals (Edinger 1942), Macrini et al. (2007b) used two characters related to the dimensions of this structure in their phylogenetic analysis. The authors stated that a hypophyseal fossa deeper (or taller) than long (depth/length $>$ 1.1) and wider than long (width/length $>$ 1.1) indicates the plesiomorphic condition for mammals, based on the distribution of these characters among non-mammalians. Thus, the specimen UFRGS-PV-1043-T presents a derived state for both characters (depth $<$ length and width $\approx$ length), differing from the non-mammalian cynodonts considered by Macrini et al. (2007b). The diversity of state characters among mammals cited by Macrini et al. (2007b) can suggest a synapomorphy for the clade involving Mammalia and *Brasilitherium* with respect to the first character (depth $<$ length) shared with monotremes and therians. On the other hand, the state of this character is reversed in some taxa (e.g., Cimolodonta and *Puchadelphys*), and is changed to another state in other therians (depth $\approx$ length). Regarding the second character, the distribution of the states makes association with phylogeny complex, because *Brasilitherium* is grouped with *Vincelestes* and some living therians (width $\approx$ length), while other derived groups of monotremes and some therians present another state (width/length $<$1.1), and the therians *Leptictis* and *Canis* present the plesiomorphic state (width/length $>$ 1.1).

There is no mark of the optic chiasm anteriorly to the hypophyseal cast. Laterally to this structure is the ventral opening of the cavum epiptericum, formed by the filling of the space between the primary and secondary walls of the skull. *Brasilitherium* presents the pattern common to all non-mammalian cynodonts, with the primary wall of the cavum, formed by an anterior extension of the prootic (i.e., the pila antotica), being medial to the semilunar ganglion of the trigeminal nerve (Presley 1980; Maier 1987 Novacek 1993; Rougier and Wible 2006). The ventral opening of the cavum epiptericum in UFRGS-PV-1043-T has a diagonal orientation, directed posterolaterally, with its longitudinal axis deviating approximately 30° from the anteroposterior axis of the endocast. On the right side of the specimen, the cast of the cavum epiptericum is incomplete, because parts of the quadrate rami of the pterygoid and alisphenoid are broken. In turn, the ventral opening of the cavum epiptericum is complete on the left side, with a maximum length of 4.67 mm and a maximum width of 2.29 mm, measured at approximately half its anteroposterior length.

Posteriorly to the hypophyseal cast, between the areas of the cava epipterica, the ventral surface of the endocast gently slopes posterodorsally (approximately 37° to the horizontal plane of the braincase) up to the line of the posterior limit of the cava epipterica. The region posterior to the cava epipterica to the foramen magnum has a rounded surface, with a more pronounced bulge along a central longitudinal band, which is aligned with the center of the foramen magnum. This region represents the ventral surface of the hindbrain and surrounding tissues (mainly meninges), and cannot specifically identify the medulla oblongata and the pons. Laterally to this region, on each side of the endocast, the filling of two foramina of the internal acoustic meatus is observed. These foramina are aligned anterioposteriorly, with the anterior foramen most likely to passage the facial nerve (VII) and the posterior

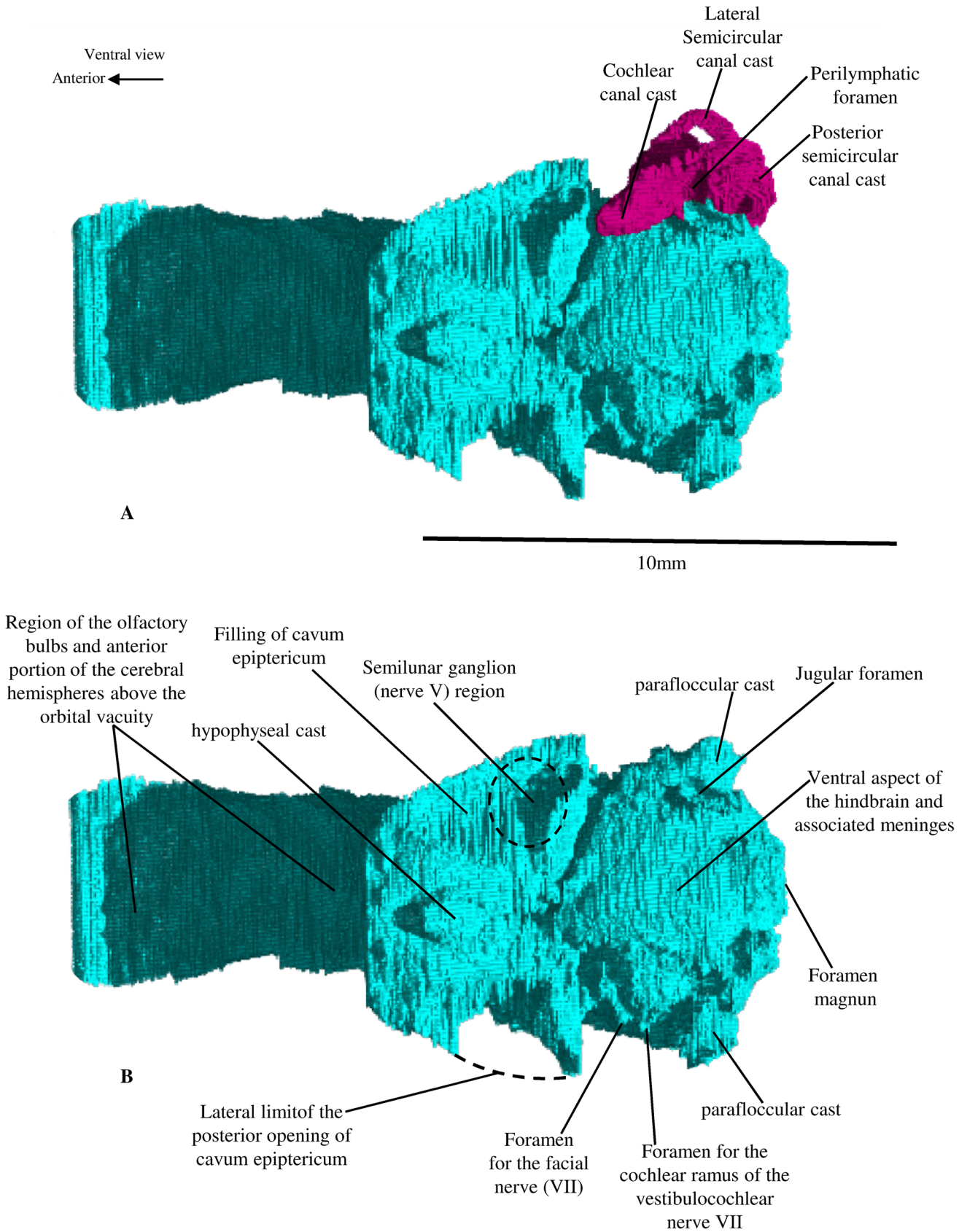

Fig. 8 Digital endocast of *Brasilitherium* UFRGS-PV-1043-T in ventral view. **a** Shows the left inner ear cast (*purple*), which was digitally removed in **b**

foramen to passage the cochlear ramus of the vestibulocochlear nerve (VIII).

Forebrain region

The most anterior part of the endocranial cast represents the space occupied by the olfactory bulbs and associated meninges (Macrini et al. 2007b). Due to the absence of an ossified cribriform plate in the skull, which separates the nasal cavity from the braincase, the exact anterior limit of the olfactory bulbs cannot be identified accurately. However, it is possible to establish an approximation of their anterior contour based on the oval shape of the casts of each bulb in dorsal view and their anteroposteriorly convex dorsal surface shape in lateral view. Furthermore, while the dorsal surface of the frontal bones (which are positioned just above this region) is flat, the ventral wall of the cast of each bulb is concave. As a result, there is a prominent division between the bulb casts, with a longitudinal groove separating the two structures. There are no visible marks suggesting the presence of accessory olfactory bulb casts in the posterior part of this region, as described for the stem therian *Vincelestes* (Macrini et al. 2007b) and the eutherian *Kennalestes* (Kielan-Jaworowska 1984), both of the Cretaceous, but these structures are often not represented in endocasts, even in living mammals (e.g., Bauchot and Stephan 1967; Jerison 1973).

The olfactory bulb casts of *Brasilitherium* UFRGS-PV-1043-T in dorsal view are two oval anteroposteriorly elongated structures (Fig. 4), with the maximum width to length ratios equal to 0.39 and 0.37 for the left and right bulb casts, respectively. The maximum width of the two olfactory bulb casts together is 4.62 mm, measured at half the length of the bulb casts, while the width on the point of the endocast immediately posterior to the dorsal bulging of the bulb casts is 3.39 mm. Comparing the endocasts of different non-mammalian cynodonts, Kielan-Jaworowska et al. (2004) indicated that the olfactory bulb casts are more developed and better separated from each other in the non-mammaliaform eucynodonts *Probelesodon* and *Massetognathus* than in *Thrinaxodon*. For *Brasilitherium*, a clear separation between the bulb casts is observed.

In addition, the length of the dorsal surface of the two olfactory bulb casts (6.10 mm) corresponds to 34.5 % of the length of the dorsal surface of the whole endocranial cast (17.67 mm), which indicates an antero-posterior expansion of the olfactory bulbs. Thus, it is apparent that these structures occupy a greater proportion of the endocranial space in *Brasilitherium* compared with other non-mammaliaform cynodonts such as *Probainognathus*, *Probelesodon*, and *Massetognathus* (Quiroga 1979, 1980a, b, c). This proportion is even higher (48 %) in UFRGS-PV-1043-T if the length of the olfactory bulb region and the whole endocast are considered, measured from the estimated anterior limit of the olfactory bulbs (9.04 mm and 18.84 mm, respectively).

With respect to the volume of the olfactory bulb casts, as already mentioned, the absence of an ossified floor for the olfactory bulbs in *Brasilitherium*, despite the presence of an ossified orbitosphenoid (indicated by Bonaparte et al. 2005), prevents accurate volumetric measurement of the olfactory bulb casts. For this reason, the volume of the olfactory bulb casts was estimated assuming that the bulbs were dorsoventrally symmetrical. Thus, the estimated volume for the region of the olfactory bulbs (135.5 mm^3) corresponds to 35.8 % of the estimated volume of the endocranial cast. Macrini et al. (2007b) used the relation between the size of the olfactory bulb casts and the total volume of the endocranial cast as a character in their phylogenetic analysis. They defined the states discreetly, with reference to an average of 6 %, with the primitive state corresponding to a size greater than or equal to 6 %. According to the volumetric data presented by Quiroga (1980b), this primitive state is observed in non-mammalian cynodonts in general, although with great variation, which would indicate more than two states for this character when taking into account these taxa. According to the work of Quiroga (1980b), the volume of the olfactory bulbs corresponds to 5 % of the endocranial cast in *Massetognathus*, 19.7 % in *Exaeretodon*, 7.8 % in *Probelesodon*, and 6.4 % in *Probainognathus*, all of them much smaller than that estimated for *Brasilitherium*.

Also, due to the lack of an ossified floor in the most anterior region of the skull, there is no impression of projections from the olfactory bulbs to the telencephalon, the olfactory tracts (Butler and Hodos 1996). However, the olfactory tracts do not usually leave impressions in endocasts of mammals, because they are hidden by the meninges (Macrini et al. 2007b). In endocasts of *Massetognathus* (Quiroga 1979, 1980c) and *Exaeretodon* (Bonaparte 1966), the olfactory tracts form a peduncle between the olfactory bulb casts and the region of the cerebral hemispheres, and thus, these two regions are separated, as found in many living reptiles (Hopson 1979; Kielan-Jaworowska et al. 2004).

The olfactory bulb casts of UFRGS-PV-1043-T are separated from the rest of the endocranial cast by a flat area that is lower than the convex surface of the bulb casts in lateral view. This is the area of the circular fissure (sensu Loo 1930; Rowe 1996), also called transverse furrow (sensu Kielan-Jaworowska 1986), transverse sulcus (sensu Krause and Kielan-Jaworowska 1993), or circular sulcus (sensu Luo et al. 2002). In dorsal view, however, the existence of a medial constriction in the dorsal aspect of the endocast remains ambiguous, because this area has a width similar to the region immediately posterior to it (the most anterior part of the cerebral hemispheres). A

well-defined circular fissure, although usually present in mammals (Macrini et al. 2007b), is not described for other non-mammalian cynodonts (Quiroga 1979, 1980a, b, c).

The dorsal surface of the endocast of UFRGS-PV-1043-T, posterior to the olfactory bulbs, is flat for an extension of 1 mm. It is thus possible to observe a longitudinal groove dividing the endocast into two laterally convex structures, which correspond to the cerebral hemispheres (Fig. 4). However, this area of the endocast is not clear, due to the presence of a transverse fracture positioned slightly in front of the posterior limit of the frontal bones and the anterior limit of the ascending process of the alisphenoid. This fracture is visible on the dorsal and lateral surfaces of the endocast and has a thickness of 0.4 mm (Figs. 4, 5). Posterior to the fracture, the bulging on each side of the groove gradually becomes clearer, and consequently, the groove becomes deeper. This groove should represent the median sulcus (=longitudinal fissure), which divides the cortex into two distinct hemispheres. The presence of two distinct hemispheres is also described for *Probainognathus* (Quiroga 1980a, b), while other non-mammaliaform cynodonts, such as *Thrinaxodon* (Kielan-Jaworowska et al. 2004), *Massetognathus* (Quiroga 1979, 1980c), *Exaeretodon* (Bonaparte 1966), and *Probelesodon* (Quiroga 1979, 1980c), do not present a division in this region of the endocast. The median sulcus is very pronounced in *Brasilitherium* throughout most of the length of the cerebral hemispheres, but it is not so deep as to indicate the presence of an ossified falx cerebri (the portion of the dura matter between the cerebral hemispheres), as is reported for different lineages of living mammals (e.g., Macrini et al. 2007b). This mark on the endocast of *Brasilitherium* should only be caused by the concave ventral surfaces of the parietal bones.

The dorsal surface of the region of the cerebral hemispheres in UFRGSPV-1043-T is 9.23 mm in length from its most anterior limit (the point where it is possible to identify the median groove between bulging of the hemispheres) to the end of the posterior slope, visible in lateral view (Fig. 5). In dorsal view, it is observed that the hemispheres in this posterior slope diverge slightly from the midline, and the median sulcus gradually becomes less prominent (Fig. 4). Considering the cerebral hemisphere casts together, the dorsal surface becomes gradually wider from its anterior limit (width = 3.60 mm) to the point of maximum width (5.21 mm) immediately anterior to the paraflocculus casts. From this point, the region of the cerebral hemispheres gradually becomes narrower until its posterior limit (width = 4.61 mm). Furthermore, due to the ventrolateral inclination of the lateral surfaces of the cerebral hemispheres, the maximum width of this region can be considered 5.80 mm at a point immediately anterior to the paraflocculus casts and below the impression of the ascending rami of the arteria and vena diploëtica magna on each side. The length to width ratio of the region of the cerebral hemispheres together varies from 2.56 to 2.00, taking into account the dorsal surface, and is 1.91 if we consider the maximum width below the vascular impressions cited above.

Anterior to the point of maximum width of the cerebral hemispheres, the endocast of *Brasilitherium* is compressed on the left side, as shown in Fig. 4. In dorsal view, the filling of the cavum epiptericum's ventral opening can be observed at this side of the endocast. The most likely shape of this structure, without post-mortem distortion, is shown in Fig. 6b, where the left and right sides of the endocast are represented with the same dimensions.

There are no markings indicating the presence of cerebral gyri and sulci [the convolutions of the cortex and the grooves between the gyri, respectively (Butler and Hodos 1996)] in the *Brasilitherium* endocast. In fact, despite the possibility that endocasts do not reflect the convolutions of the real brains [e.g., *Tursiops truncatus* (Colbert et al. 2005)], it is expected that non-mammalian cynodonts have lissencephalic surfaces (smooth cortical brain surfaces) because this condition is considered plesiomorphic for the mammalian crown-group (Kielan-Jaworowska et al. 2004).

Also, there is no mark indicating a pineal body on the dorsal surface of the endocast of UFRGS-PV-1043-T. The pineal body and the associated parietal eye include the portion of the epithalamus (Butler and Hodos 1996) of the diencephalon, having thermoreceptive functions that regulate circadian rhythms and reproductive cycles (Roth et al. 1986; Butler and Hodos 1996). In fact, the parietal foramen (opening to the parietal eye) is absent in most eucynodonts [but is present in *Cynognathus*, *Pascualgnathus*, and *Diademodon* (e.g., Bonaparte et al. 2005; Abdala 2007)]. Without a parietal eye, the pineal body leaves little or no bone marks to be identified in endocasts (Roth et al. 1986). Nevertheless, despite the absence of the parietal foramen, a cast of a parietal tube is indicated in the parietal endocranial cast of *Massetognathus* (Quiroga 1979, 1980c). Moreover, Quiroga (1980b, c) suggested a pineal region in the endocast of *Probainognathus* behind the median sulcus at the most posterior region of the cerebral hemispheres, where they diverge. In any case, the endocast of *Brasilitherium* neither presents a space significantly wider than the median sulcus in the most posterior portion of the hemispheres, nor a parietal tube.

The ventral boundary of the telencephalon, separating this region from the rest of the endocast, cannot be accurately determined in *Brasilitherium* UFRGS-PV-1043-T, nor can the boundary of the isocortex (neocortex), i.e., the rhinal fissure. However, this latter feature can be present in brains without appearing in the respective endocasts (Jerison 1991). Moreover, the lack of a rhinal fissure can also be associated with the small brain sizes of some mammals

(Rowe 1996). Nevertheless, a rhinal fissure is not described for other non-mammalian cynodonts, being present only among taxa of the mammalian crown-group (Macrini et al. 2007b). The presence of a neocortex (isocortex) in *Probainognathus* was suggested by Quiroga (1980b), based on the presence of a groove that would mark the posterior limit of that region. However, this interpretation has been contested by Kielan-Jaworowska (1986), who considered such groove the mark of a blood vessel in the external surface of the brain.

Midbrain region

The portion of the midbrain exposed on the dorsal surface of endocasts generally corresponds mainly to the anterior and posterior colliculi. However, the midbrain may not be visible in endocasts if it is covered by meninges and associated blood sinuses, or if there is a posteriorly expanded telencephalon or an anteriorly expanded cerebellum (Edinger 1964). Moreover, the structures of the midbrain may be exposed on the dorsal surface of the brain without appearing in endocasts, even in living taxa, as is the case of *Didelphis virginiana* (Dom et al. 1970), *Monodelphis domestica* (Macrini et al. 2007a), and *Tenrec ecaudatus* (Bauchot and Stephan 1967).

In *Brasilitherium* UFRGS-PV-1043-T, the dorsal surface of the endocast appears to be continuous from the anterior limit of the cerebral hemisphere casts to the end of the slope in the posterior direction in front of the lower cerebellar region. Thus, there is no evidence of exposure of the midbrain on the dorsal surface of the endocast. Even so, it cannot be ruled out that the midbrain has been partially exposed on the dorsal surface of the actual brain of *Brasilitherium*, and their endocasts may not present a midbrain mark due to the presence of meninges. In this case, the posterior limit of the cerebral hemispheres could be located immediately anterior to the observed slope in front of the cerebellar region, or in any part of this slope, where the median sulcus becomes less prominent. On the other hand, if the endocast represents the dorsal surface of the actual brain in this region, the midbrain will likely have been covered by a telencephalon (see Fig. 5c), because the casts of the dorsal surface of the cerebral hemispheres appear to extend to the cerebellar region.

The presence of casts of these structures has been described for several extinct mammals, e.g., *Labidolemur* (Silcox et al. 2011), *Kennalestes* (Kielan-Jaworowska 1984, 1986), *Asioryctes* (Kielan-Jaworowska 1984), and *Zalambdalestes* (Kielan-Jaworowska 1984, 1986), as well as for the non-mammalian cynodont *Probainognathus* (Quiroga 1980b, c). In any case, the plesiomorphic condition for the mammalian crown-group, according to Macrini et al. (2007b), should be the non-exposure of the midbrain.

Hindbrain region

Because there is no dorsal exposure of the midbrain, the cerebral hemisphere casts (forebrain) extend posteriorly beyond the anterior limit of the fossa subarcuata, which is surrounded by the bony anterior semicircular canal and is filled by the paraflocculus lobe of the cerebellum (Figs. 4, 5). In dorsal view, immediately behind the parafloccular casts and anteriorly to the posterior limit of the cerebral hemispheres region (indicated by the end of the median sulcus), the region that presumably represents the dorsal surface of the cerebellum appears. This region is 1.3 mm in anteroposterior length and 4.2 mm in width (Fig. 4), and can be seen in side view behind the slope of the posterior region of the cerebral hemispheres (Figs. 5, 8). In dorsal view, the surface of the cerebellar region has a bulging on the left, which could suggest a cerebellar hemisphere. In addition, the dorsal surface of the cerebellum has a thin elevation along the median line, which, in turn, could correspond to the vermis of the cerebellum. However, the right side of the cerebellar region shows a deep notch (Fig. 4), which resulted from the breakage of a bone over that area, making it difficult to identify structures in this region.

In general, the cerebellar region also appears to be slightly larger in *Brasilitherium* than in *Probainognathus* (see Quiroga 1980a, b), which is the taxon with the most derived neuroanatomic features among the non-mammaliaform cynodonts with described endocasts. As the point of maximum width of the endocast for both taxa, just at the parafloccular casts, the maximum width to length ratio of the endocast reflects the relative width of the cerebellar region. This ratio is 0.4 in *Brasilitherium* UFRGS-PV-1043-T. Although Quiroga (1980a, b) did not mention these linear measurements in his works on the endocast of *Probainognathus*, the ratio 0.37 can be inferred from his figures.

The parafloccular casts are prominent in the endocast of *Brasilitherium*, especially in dorsal view, as roughly cylindrical structures with a slightly rounded apex. The parafloccular casts are laterally projected away from the rest of the endocast (1.20 and 1.32 mm, respectively, on the right and left sides). These casts are posterolaterally oriented away from the longitudinal axis of the endocranial cast by approximately 40°–60° (43° and 61°, considering the greater angle between the central axis of parafloccular cast at the left and right sides, respectively). These casts are relatively wide, with the ratio between their largest diameters close to 1.0 (1.51: 1,50 in the left side and 1,78:1.51 in the right side).

As already mentioned, the distance between the lateral limits of the two parafloccular casts corresponds to the maximum width of the endocast of *Brasilitherium*.

Together, the two paraflocular casts constitute approximately 2 % of the estimated endocast volume. The paraflocculus is associated with coordination, balance and vestibular sensory acquisition (Butler and Hodos 1996). Although the degree of filling of the fossa subarcuata can be variable in different mammals (e.g., Sánchez-Villagra 2002), this feature in endocasts is associated with the degree of development of the paraflocculi lobes (Kielan-Jaworowska et al. 2004). Paraflocular casts are absent in the endocasts of some non-therapsid cynodonts, often due to the poor ossification of this region of the skull (Kielan-Jaworowska et al. 2004). On the other hand, the presence of prominent paraflocculi is a plesiomorphic condition for eucynodonts, as described for *Thrinaxodon* (Rowe 1996), *Nythosaurus* (Hopson 1979), and all other non-eucinodont mammaliaforms with described endocasts (e.g., Quiroga 1979, 1980a, b, c).

Relative size of the brain cast

The total volume of the endocast (with the estimated ventral limit of the olfactory bulb casts, as shown in Fig. 5b) is 378.436 mm^3, or 0.378 ml (this total volume is approximately 20 % larger than the volume delimited by the ventral limit of the frontal bone above the orbital vacuity, as shown in Fig. 5a). This volume results in an EQ of 0.1475 or 0.2233 according to the equations used (Table 2), both based on a mass of 96.57 g, estimated for the specimen UFRGS-PV-1043-T. The volume given here corresponds to the endocast digitally obtained without corrections for the deformation of the specimen. Thus, the EQ value could be higher if the region of the cerebral hemispheres were larger on the left side, as suggested in Fig. 9. In the endocast used for the EQ calculations, the cava epipterica casts (removed in the images shown in Figs. 4 and 8) were maintained because these spaces in living species are occupied by nervous structures (geniculate and semilunar ganglions), and are incorporated into the cranial cavity in mammals (Goodrich 1930; Kuhn and Zeller 1987; Kielan-Jaworowska et al. 2004). Furthermore, the space filling of the cava epipterica is usually not removed in paleoneurological works of non-mammalian cynodonts (Jerison 1973; Quiroga 1979, 1980a, b).

Comparing the EQ values previously described for different cynodonts, the EQs calculated for UFRGS-PV-1043-T (Fig. 10) are below the those of mammaliaforms, suggesting a gradual increase in the relative size of the *Brasilitherium* brain, progressing to the non-mammalian mammaliaforms *Morganucodon* and *Hadrocodium* and up to the taxa of the mammalian crown-group. However, despite the observed neuroanatomical changes, there is no clear gradual encephalization among non-mammaliaform cynodonts successively more closely related to mammaliaforms, considering the EQ values reported for *Diademodon* (0.14 and 0.21) and *Massetognathus* (0.15 and 0.22) by Quiroga (1980b). The *Brasilitherium* EQ (0.15), calculated with the same equation used for other non-mammaliaform cynodonts (= 0.15) by Jerison (1973) and Quiroga (1979, 1980a, b, c), may be similar to or even lower than the EQs of these taxa, depending on the equation used for estimating the body mass. In addition to *Diademodon* and *Massetognathus*, the taxa *Probelesodon* and *Probainognathus* also appear to exceed the calculated EQ for *Brasilitherium* from the same equation used by Quiroga (1979, 1980a, b), when taking into account the EQ values the author obtained with the lowest mass estimates for those taxa (resulting in an increase in the relative size of the brain).

On the other hand, comparing the 3D reconstructions based on CT scans of *Brasilitherium* UFRGS-PV-1043-T with that of *Massetognathus pascuali* UFRGS-PV-0968-T (Fig. 10), the *Brasilitherium* endocast is proportionally larger in relation to skull size. Figure 10c shows a comparison of the space occupied by the brain in the different mammaliaform skulls according to Luo et al. (2001). Thus, the relative size of the brain endocast of *Brasilitherium* presents an intermediate condition between the *Massetognathus* sample and the non-mammalian mammaliaforms compared, being even closer to the configuration observed in the latter. In addition to the clear increase in relative size of the olfactory bulbs compared with other non-mammaliaform cynodonts, *Brasilitherium* shows a considerable enlargement in the regions of the cerebral hemispheres (especially at their most posterior part) and the cerebellum.

Discussion

First, it is important to take into account this study's limitations; because the intracranial space is also occupied by other tissues, an endocast is only an approximation of the actual brain. In addition, the absence of an ossified floor for the olfactory bulb region prevents an exact volumetric measurement of these structures and, consequently, of the whole endocast. Moreover, EQ calculation, in addition to the endocast volume, includes the body mass, which must to be estimated for fossil taxa. Even so, the endocast of specimen UFRGS-PV-1043-T exhibits marks indicating different brain structures, and the conclusions of this work are based on the observable data, as well as an estimate of the ventral contour of the olfactory bulb region. This estimate was based on the observed dorsal shape of these structures, here considered as being symmetrical to their ventral portion. Thus, it was possible to compare *Brasilitherium* with other taxa with endocasts described in the literature, and to make evolutionary inferences. With

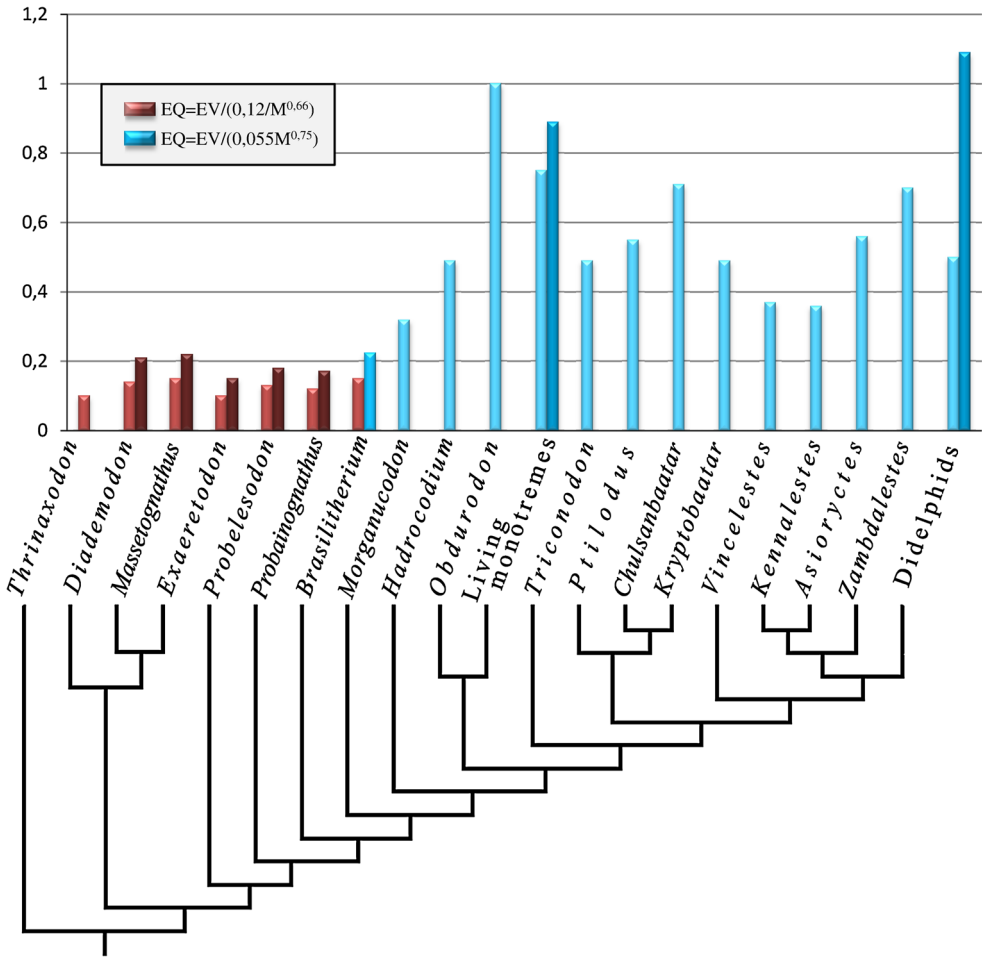

Fig. 9 Graphic comparing the Encephalization Quotient (EQ) calculated for different non-mammalian cynodonts and mammals: *Thrinaxodon*, 0.1 (Jerison 1973); *Diademodon*, 0.14 (Quiroga 1980b) and 0.21 (Jerison 1973); *Massetognathus*, 0.15 and 0.22 (Quiroga 1979, 1980b); *Exaeretodon*, 0.10 and 0.15 (Quiroga 1980b); *Probelesodon*, 0.13 and 0.18 (Quiroga 1979, 1980b); *Probainognathus*, 0.12 and 0.17 (Quiroga 1980a, b); *Brasilitherium*, 0.15 and 0.22; *Morganucodon*, 0.32 (Rowe et al. 2011); *Hadrocodium*, 0.49 (Rowe et al. 2011); *Obdurodon*, 1.00 (Macrini et al. 2007a); living monotremes 0.75 to 0.89 (Macrini et al. 2007a); *Triconodon*, 0.49 (Kielan-Jaworowska 1983); *Chulsanbaatar*, 0.55 (Kielan-Jaworowska 1983); *Kryptobaatar*, 0.71 (Kielan-Jaworowska and Lancaster 2004); *Ptilodus*, 0.49 (Kielan-Jaworowska 1983); *Vincelestes*, 0.37 (Macrini et al. 2007b); *Kennalestes*, 0.36 (Kielan-Jaworowska 1984); *Asioryctes*, 0.56 (Kielan-Jaworowska 1984); *Zambdalestes*, 0.7 (Kielan-Jaworowska 1984); and didelphids, 0.5 to 1.09 (Eisenberg and Wilson 1981). The taxa are arranged according to their phylogenetic relationships, according to the cladogram. [Based on Abdala (2007) for non-mammalian cynodonts, Wible and Rougier (2000) for the relationships among the multituberculates (*Ptilodus*, *Chulsobaatar*, *Kryptobaatar*), and Luo and Wible (2005) for other mammals]. The two EQs shown for *Brasilitherium* were obtained using different equations: EQ = EV/(0.12 $M^{0,\ 66)}$ (Jerison 1973), for comparison with other non-mammalian cynodonts, and EQ = EV/(0.055 $M^{0,\ 75)}$ (Eisenberg 1981), for mammals (EV being the volume of the brain or the endocast and M being body mass). The two EQ values for other non-mammalian cynodonts are due to different estimates of body mass using two different equations (see Quiroga 1980b), while the two values for living monotremes and didelphids represent the limits of the EQ ranges among the different taxa of these groups. Jerison (1973) arbitrarily excluded the cast of the olfactory bulbs of *Thrinaxodon* and *Diademodon* from the endocast volume, while Quiroga (1979, 1980b) discounted the percentage of the endocast volumes, with the exception of *Probainognathus*, considering the space occupied by meninges in *Diademodon* (−20 %), *Exaeretodon* (−15 %), *Massetognathus* (−10 %), and *Probelesoson* (−10 %)

respect to the body mass estimated, we used the same equation for *Brasilitherium* utilized for small non-mammalian mammaliaforms by Luo et al. (2001), whose reported EQs are used here comparatively. Furthermore, the EQ calculated for *Brasilitherium* appears to be consistent with the neuroanatomical features observed, and with its likely phylogenetic relationship with some non-mammalian mammaliaforms.

In general, the digital endocast obtained from specimen UFRGS-PV-1043-T does not differ significantly from those of other non-mammaliaform cynodonts. Even so, some neuroanatomical changes can be identified among these taxa as they become more closely related to mammaliaforms, such as the absence of the parietal eye in most eucynodonts and a gradual increase in the width of the cerebral hemisphere region, especially in their posterior

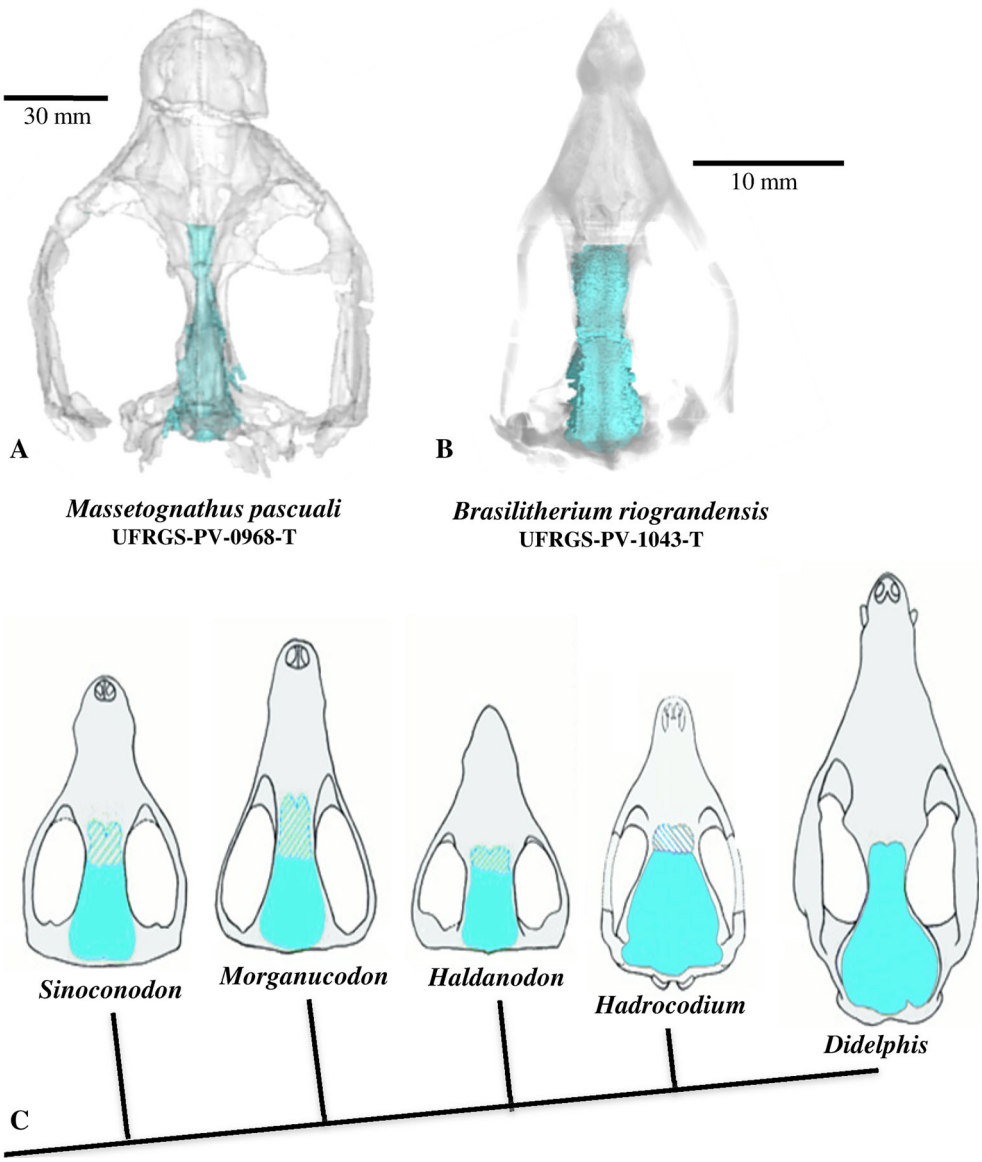

Fig. 10 Space occupied by the brain in the skulls of different cynodont taxa. 3D reconstructions from CT scan images of the skulls of *Massetognathus*, UFRGS-PV-0968-T (**a**), and *Brasilitherium*, UFRGS-PV-0929-T (**b**) in dorsal view, with the bony elements appearing in semi-transparence to highlight the blue endocast. **c** Shows representations of the skulls of five Mammaliaformes (not to scale), arranged according to their phylogenetic relationships and aligned at the site of the cranio-mandibular joint, with the relative brain size represented in *blue* (modified from Luo et al. 2001)

parts. *Probainognathus* (Quiroga 1980a, b) presents cerebral hemisphere casts that are clearly divided, and wider than those of *Thrinaxodon* (Kielan-Jaworowska et al. 2004), *Massetognathus* (Quiroga 1979, 1980c), *Exaeretodon* (Bonaparte 1966), and *Probelesodon* (Quiroga 1979, 1980c). *Brasilitherium* is even more derivated in these features than *Probainognathus*. Moreover, contrary to what is described for *Probainognathus* by Quiroga (1980a, b), *Brasilitherium* most likely had no dorsal exposure of the midbrain and pineal body. Although the dorsal exposure of the midbrain may represent a primitive condition for placentals (Kielan-Jaworowska et al. 2004; Silcox et al. 2011), this character is also plesiomorphic for the mammalian crown-group (Macrini et al. 2007b). Among non-mammaliaform cynodonts, we can consider that the condition of *Brasilitherium* was most likely associated with an increase of the cerebral hemispheres, which covered the colliculus, extending posteriorly to the anterior limit of the cerebellar region.

The width of the cerebellar region also appears to have gradually increased through an evolutionary sequence among non-mammaliaform cynodonts successively more closely related to mammaliaforms, with *Brasilitherium* slightly more advanced than *Probainognathus*, as derived in comparison to *Thrinaxodon* (Kielan-Jaworowska et al. 2004), *Massetognathus* (Quiroga 1979, 1980c), *Exaeretodon* (Bonaparte 1966) and *Probelesodon* (Quiroga 1979, 1980c). However, the enlargement of the cerebral hemispheres and the cerebellar region, which can be observed in *Brasilitherium* in comparison with other non-mammaliaform cynodonts, is significantly less pronounced than in *Morganucodon* and other mammaliaforms (see Fig. 10).

The most outstanding neuroanatomical characteristic, considering the endocast of *Brasilitherium* under an evolutionary perspective from non-mammalian cynodonts to mammals, seems to be the relative size of the olfactory bulbs. The olfactory bulb casts become more conspicuous and have a more distinct division in some eucynodonts, such as *Probelesodon* and *Massetognathus*, but in *Brasilitherium*, these structures become even more developed. This fact can be visually verified by taking into account the length of the dorsal surface of the olfactory bulb region in relation to the endocast length in *Brasilitherium* compared with non-mammaliaform cynodonts such as *Probainognathus*, *Probelesodon*, and *Massetognathus* (Quiroga 1979, 1980a, b, c). Compared with non-mammalian mammaliaforms, the olfactory bulb region in *Brasilitherium* is larger (see Fig. 10 for an example), perhaps because of the enlargement of the cerebral hemispheres observed in mammaliaforms.

Moreover, it is possible to make a quantitative comparison between *Brasilitherium* and other taxa from the literature, based on the volume of the olfactory bulb casts in relation to the whole endocast. In this sense, the percentage of the estimated volume of the endocast corresponding to the olfactory bulb casts in *Brasilitherium* UFRGS-PV-1043-T (35.8 %) is higher than in other non-mammaliaform cynodonts, according to data presented by Quiroga (1980b). Although *Probainognathus* is more closely related to *Brasilitherium* and mammaliaforms, there is little difference between the percentages of *Probainognathus* (6.4 %) and *Probelesodon* (7.8 %), and between both them and *Massetognathus* (5 %). This result suggests that *Brasilitherium* may represent a derived state, with significantly larger olfactory bulbs, whose lengths also correspond to more than 30 % of the length of the endocast. The hypothesis of a trend toward an increase in the relative size of olfactory bulbs is also supported by observations of the endocasts of the non-mammalian mammaliaforms *Morganucodon* and *Hadrocodium* presented by Rowe et al. (2011). These taxa are mentioned by the authors as examples of two "pulses" of encephalization in mammalian brain evolution, with still a third pulse represented by the mammalian crown-group. However, these pulses are determined by a significant widening in the region of the cerebral hemispheres and cerebellum. Consequently, although Kielan-Jaworowska et al. (2004) cited a greater extent of ventral olfactory bulbs in mammaliaforms, it is likely that they account for a smaller percentage of the brain compared with *Brasilitherium*. Thus, this taxon may present the largest olfactory bulbs among all known cynodonts, and the growth of these structures preceded a most significant enlargement of the rest of the brain, which is observed only in mammaliaforms.

In addition, the slight enlargement of the region of the cerebral hemispheres and, mainly, the development of the olfactory bulbs in *Brasilitherium* could suggest an EQ higher than other non-mammaliaform cynodonts, but such a difference is not confirmed by comparing all EQ values reported for these taxa. Using the same equation to calculate the EQ used for other non-mammaliaform cynodonts, the EQ of *Brasilitherium* has values similar to or even lower than *Diademodon* and *Massetognathus*, as well as *Probelesodon* and *Probainognathus*, depending on the equation used to estimate the masses of these taxa. Furthermore, Quiroga (1979, 1980b) also subtracted arbitrarily defined percentages between 10 and 20 % from the endocast volumes of the cynodonts studied to deduce the volume of the meninges. Thus, the EQ values could be even greater.

However, by visually comparing the endocasts of *Brasilitherium* and other cynodonts in Fig. 10, it is clear that the endocast of the taxon described here is greater in relation to the skull compared with *Massetognathus*, suggesting that the EQs of *Diademodon* and *Massetognathus* may have been overestimated in the equation used to estimate the body mass. Alternatively, the EQ of *Brasilitherium* could have been underestimated (due to an overestimated body mass or an underestimated volume of the olfactory bulb casts). Nevertheless, with the same estimated mass and using the same equation for calculating EQ used by Rowe et al. (2011) for *Morganucodon* (EQ = 0.32) and *Hadrocodium* (EQ = 0.49), the value obtained for *Brasilitherium* UFRGS-PV-1043-T (=0.22) seems to agree with an evolutionary sequence from values <0.20 for non-mammaliamorph cynodonts to increasing EQs in the taxa more closely related to mammals.

A trend of encephalization increase initially associated with an enhancement in olfactory accuracy was also studied by Rowe et al. (2011). These authors noted the improvement in neuromuscular coordination and tactile sensitivity through hairs to infer the presence of a neocortex in *Morganucodon* and *Hadrocodium*. This assumption is based on the impressions of a thick coat reported for the non-mammalian mammaliaform *C. lutrasimilis* (Ji et al. 2006), given the predominance of initial somatosensory mechanoreceptors associated with skin, hair follicles and proprioceptors in the neocortex. According to Rowe et al. (2011), the origin of the mammalian crown-group marks the third pulse of olfactory development, with ossified ethmoturbinals, a cribriform plate and a rigid support in the nasal cavity for the olfactory epithelium receptor (OR). In turn, the activation of OR genes, which in mammals exceed those in the genomes of most other vertebrates by approximately one order of magnitude (Niimura 2009), induces growth of the olfactory epithelium and turbinates, as well as their ossification (Rowe et al. 2005). According

to these authors, the elaborate visual and auditory systems of mammals evolved later than these olfactory improvements.

For *Brasilitherium*, the presence of coat coverage can be inferred by considering its likely endothermy (Rodrigues 2005; Rodrigues and Schultz 2005; Rodrigues et al. 2006) and small size. Both factors imply a high surface/volume ratio and, therefore, greater endogenous heat dissipation, which would worsen in the case of a nocturnal habit, as is assumed (e.g., Jerison 1973; Kielan-Jaworowska et al. 2004). Some degree of endothermy would already be a plesiomorphic feature for eucynodonts, with the closure of the secondary palate providing a cross-sectional nasal cavity area (in the coronal plane in relation to the skull) large enough to house respiratory turbinates (Hillenius 1992; Ruben et al. 1996; 2003). In addition, bony ridges were found on the medial surface of the maxillar bone, where the turbinals should be inserted in different non-mammaliaform epicynodonts (Hillenius 1994; Rodrigues 2005; Rodrigues et al. 2006). Reinforcing this hypothesis, the 3D reconstruction of the specimen UFRGS-PV-1043-T in the present study allowed the observation of turbinal structures (publication in preparation). Therefore, poorly developed respiratory turbinals ridges in *Thrinaxodon* and other non-mammalian cynodonts compared with the crown-group Mammalia (e.g., Kielan-Jaworowska et al. 2004) could indicate that the turbinals themselves would become more developed and ossified in association with increased metabolic rates along the Mammalia stemline evolution. Thus, *Brasilitherium* could already have had metabolic rates and a body temperature closer to the mammalian pattern.

Even so, we do not suggest the presence of a neocortex in *Brasilitherium* due to a lack of direct evidence. Also, it cannot be ruled out that the animal, even being endothermic and having a small size, did not need the thermal insulation for the temperature range of the environment where it lived. In addition, Rowe et al. (2011) stated that, ontogenetically, the hairs initially had a sensory function before acquiring an isolation function with the maturation of thermoregulation. However, we cannot say that the early evolution of the coat had a direct correspondence with the development of the neocortex in the brain. Moreover, aside from the lack of the rhinal fissure on the endocast, a character that is also absent in *Morganucodon* and *Hadrocodium*, the enlargement of the cerebral hemisphere region observed in UFRGS-PV-1043-T is highly incipient compared with that observed in mammaliaforms. Regarding the development of the brain (especially in relation to olfaction), due to the presence of ossified maxilloturbinals in *Brasilitherium* (publication in preparation), it may have been possible for this taxon to develop turbinates in the whole nasal cavity, including its more posterior region, with olfactory function. These turbinals were most likely not fully ossified, but could still support a greater epithelial surface with olfactory receptors in association with the observed development of the olfactory bulbs. Thus, we can suggest that the adaptations for olfactory reception seem to have been associated with a process of encephalization even before the origin of the Mammaliaformes. This evolutionary process seems to have been initiated by the increase of the olfactory bulbs in association with the changes in the nasal cavity related to endothermy and olfaction acuity, before the more expressive enlargement of the cerebral hemispheres observed in the mammaliaforms.

Acknowledgments The fieldwork for data collection was supported by the National Geographic Society and the Ligabue Foundation of Venice (Italy). The specimen was prepared by José Fernando Bonaparte (UFRGS/NGS) and Agustin Martinelli (Sección Paleontología de Vertebrados, Museo Argentino de Ciencias Naturales "Bernardino Rivadavia"), and was taken to Germany by JFB to be scanned at the Hochschule Aalen through a project submitted to the Alexander von Humboldt Foundation with the participation of Wolfgang Maier (Institut für Evolution und Ökologie, Eberhard-Karls-Universität Tübingen).

References

Abdala, F. 2007. Redescription of *Platycraniellus elegans* (Therapsida, Cynodontia) from the Lower Triassic of South Africa, and the cladistic relationships of eutheriodonts. *Palaeontology* 50(3): 591–618.

Bauchot, R., and H. Stephan. 1966. Données nouvelles sur l'encéphalisation des insectivores et des prosimiens. *Mammalia* 30: 160–196.

Bauchot, R., and H. Stephan. 1967. Encephales et moulages endocraniens de quelque insectivores et primates actuels. *Colloques Internationaux du Centre National de la Recherche Scientifique* 163: 575–587.

Bonaparte, J.F. 1966. Sobre las cavidades cerebral, nasal y otras estructuras del craneo de *Exaeretodon* sp. (Cynodontia-Traversodontidae). *Acta Geologica Lilloana* 8: 5–11.

Bonaparte, J.F., A.G. Martinelli, C.L. Schultz, and R. Rupert. 2003. The sister group of mammals: small cynodonts from the late Triassic of southern Brazil. *Revista Brasileira de Paleontologia* 5: 5–27.

Bonaparte, J.F., A.G. Martinelli, and C.L. Schultz. 2005. New information on *Brasilodon* and *Brasilitherium* (Cynodontia, Probainognathia) from the Late Triassic of Southern Brazil. *Revista Brasileira de Paleontologia* 8(1): 25–46.

Butler, A.B., and W. Hodos. 1996. *Comparative Vertebrate Neuroanatomy: Evolution and Adaptation*. New York: Wiley-Liss.

Colbert, M.W., R. Racicot, and T. Rowe. 2005. Anatomy of the cranial endocast of the bottlenose dolphin *Tursiops truncatus*, based on HRXCT. *Journal of Mammalian Evolution* 12: 195–207.

Deacon, T.W. 1990. Rethinking mammalian brain evolution. *American Zoologist* 30: 629–705.

Dom, R., B.L. Fisher, and G.F. Martin. 1970. The venous system of the head and neck of the opossum (*Didelphis virginiana*). *Journal of Morphology* 132: 487–496.

Dunbar, R.I.M. 1995. Neocortex size and group size in primates: a test of the hypothesis. *Journal of Human Evolution* 28: 287–296.

Edinger, T. 1942. The pituitary body in giant animals fossil and living: a survey and a suggestion. *Quarterly Review of Biology* 17: 31–45.

Edinger, T. 1948. Evolution of the horse brain. *Geological Society of America Memoir* 25: 1–177.

Edinger, T. 1955. Hearing and smell in cetacean history. *Monatsschrift für Psychiatrie und Neurologie* 129: 37–58.

Edinger, T. 1964. Midbrain exposure and overlap in mammals. *American Zoologist* 4: 5–19.

Eisenberg, J.F. 1981. *The Mammalian Radiations*. Chicago: University of Chicago.

Eisenberg, J.F., and D.E. Wilson. 1978. Relative brain size and feeding strategies in the Chiroptera. *Evolution* 32: 740–751.

Eisenberg, J.F., and D.E. Wilson. 1981. Relative brain size and demographic strategies in *Didelphis marsupialis*. *American Naturalist* 118: 1–15.

Gingerich, P.D., and B.H. Smith. 1984. Allometric scaling in the dentition of primates and insectivores. In *Size and Scaling in Primate Biology*, ed. W.L. Jungers, 257–272. New York: Plenum Press.

Goodrich, E.S. 1930. *Studies on the Structure and Development of the Vertebrates*. London: Macmillan and Co. Ltd.

Hillenius, W.J. 1992. The evolution of nasal turbinates and mammalian endothermy. *Paleobiology* 18: 17–29.

Hillenius, W.J. 1994. Turbinates in therapsids: evidence for Late Permian origins of mammalian endothermy. *Evolution* 48: 207–229.

Hopson, J.A. 1979. Paleoneurology. In *Biology of the Reptilia, Volume 9, Neurology A*, ed. C. Gans, R.G. Northcutt, and P. Ulinski, 39–146. London: Academic Press.

Hopson, J.A., and Kitching, J.W. 2001. A probainognathian cynodont from South Africa and the phylogeny of nonmammalian cynodonts. In *Studies in Organismic and Evolutionary Biology in Honor of Alfred W. Crompton—Bulletin of Museum of Comparative Zoology*, vol. 156, eds. F.A. Jenkins, M.D. Shapiro, and T. Owerkowicz, 5–35.

Jerison, H.J. 1973. *Evolution of the Brain and Intelligence*. New York: Academic Press.

Jerison, H.J. 1991. Fossil brains and the evolution of the neocortex. In *The Neocortex: Ontogeny and Phylogeny. NATO Advanced Science Institutes Series A: Life Sciences* vol. 200, eds. B.L. Finlay, G. Innocenti, and H. Scheich. New York: Plenum Press.

Ji, Q., Z.-X. Luo, C.-X. Yuan, and A.R. Tabrum. 2006. A swimming mammaliaform from the Middle Jurassic and ecomorphological diversification of early mammals. *Science* 311: 1123–1127.

Kemp, T.S. 1979. The primitive cynodont *Procynosuchus*: structure, function, and evolution of the postcranial skeleton. *Philosophical Transactions of the Royal Society of London. Series B* 288: 217–258.

Kemp, T.S. 2009. The endocranial cavity of a nonmammalian cynodonts *Chiniquodon theotenicus* and its implications for the origin of the mammalian brain. *Journal of Vertebrate Paleontology* 29(4): 1188–1198.

Kermack, K.A., F. Mussett, and H.W. Rigney. 1981. The skull of *Morganucodon*. *Zoological Journal of the Linnean Society* 53: 87–175.

Kielan-Jaworowska, Z. 1983. Multituberculate endocranial casts. *Palaeovertebrata* 13: 1–12.

Kielan-Jaworowska, Z. 1984. Evolution of the therian mammals in the late Cretaceous of Asia. Part VI. Endocranial casts of eutherian mammals. *Palaeontologia Polonica* 46: 157–171.

Kielan-Jaworowska, Z. 1986. Brain evolution in Mesozoic mammals. In *Vertebrates, Phylogeny, and Philosophy. Contributions to Geology, University of Wyoming, Special Paper 3*, eds. K.M. Flanagan, and J.A. Lillegraven, 21–34.

Kielan-Jaworowska, Z. 1997. Characters of multituberculates neglected in phylogenetic analyses of early mammals. *Lethaia* 29: 249–266.

Kielan-Jaworowska, Z., R.L. Cifelli, and Z.-X. Luo. 2004. *Mammals from the Age of Dinosaurs: Origin, Evolution, and Structure*. New York: Columbia University Press.

Kielan-Jaworowska, Z., and T.E. Lancaster. 2004. A new reconstruction of multituberculate endocranial casts and encephalization quotient of *Kryptobaatar*. *Acta Palaeontologica Polonica* 49: 177–188.

Krause, D.W., and Z. Kielan-Jaworowska. 1993. The endocranial cast and encephalization quotient of *Ptilodus* (Multituberculata, Mammalia). *Palaeovertebrata* 22: 99–112.

Kuhn, H., and U. Zeller. 1987. The cavum epiptericum in monotremes and therian mammals. In *Morphogenesis of the mammalian skull*, ed. U. Zeller, and H. Kuhn, 51–70. Berlin: Parey.

Liu, J., and P. Olsen. 2010. The phylogenetic relationships of Eucynodontia (Amniota: Synapsida). *Journal of Mammalian Evolution* 17: 151–176.

Loo, Y.T. 1930. The forebrain of the opossum, *Didelphis virginiana*. *Journal of Comparative Neurology* 51: 13–64.

Luo, Z.-X., A.W. Crompton, and A.-L. Sun. 2001. A new mammaliaform from the early Jurassic and evolution of mammalian characteristics. *Science* 292: 1535–1540.

Luo, Z.-X., Z. Kielan-Jaworowska, and R.L. Cifelli. 2002. In quest for a phylogeny of Mesozoic mammals. *Acta Palaeontologica Polonica* 47: 1–78.

Luo, Z.-X., and J.R. Wible. 2005. A late Jurassic digging mammal and early mammalian diversity. *Science* 308: 103–107.

Macrini, T.E., C. Muizon, R.L. Cifelli, and T. Rowe. 2007a. Digital cranial endocast of *Pucadelphys andinus*, a Paleocene metatherian. *Journal of Vertebrate Paleontology* 27: 99–107.

Macrini, T.E., G.W. Rougier, and T. Rowe. 2007b. Description of a cranial endocast from the fossil mammal *Vincelestes neuquenianus* (Theriiformes) and its relevance to the evolution of endocranial characters in therians. *The Anatomical record* 290(7): 875–892.

Macrini, T.E., T. Rowe, and M. Archer. 2006. Description of a cranial endocast from a fossil platypus, *Obdurodon dicksoni* (Monotremata, Ornithorhynchidae), and the relevance of endocranial characters to monotreme monophyly. *Journal of Morphology* 267: 1000–1015.

Maier, W. 1987. The ontogenetic development of the orbitotemporal region of the skull of *Monodelphis domestica* (Didelphidae, Marsupialia), and the problem of the mammalian alisphenoid. *Mammalia Depicta* 13: 71–90.

Nieuwenhuys, R., H.J. Donkelaar, and C. Nicholson. 1998. *The central nervous system of vertebrates*. Berlin: Springer.

Niimura, Y. 2009. On the origin and evolution of vertebrate olfactory receptor genes: comparative genome analysis among 23 chordate species. *Genome Biology and Evolution* 1: 34–44.

Novacek, M.J. 1986. The skull of leptictid insectivorans and the higher-level classification of eutherian mammals. *Bulletin of the American Museum of Natural History* 183(1): 1–111.

Novacek, M.J. 1993. Mammalian phylogeny: morphology and molecules. *Trends in Ecology and Evolution* 8(9): 339–340.

Presley, R. 1980. The braincase in Recent and Mesozoic therapsids. *Mémoires, Société Géologique de France N.S.*, 139: 159–162.

Quiroga, J.C. 1979. The brain of two mammal-like reptiles (Cynodontia- Therapsida). *Journal für Hirnforschung* 20: 341–350.

Quiroga, J.C. 1980a. Sobre un molde endocraneano del cinodonte *Probainognathus jenseni* Romer, 1970 (Reptilia, Therapsida), de la Formación Ischichuca (Triasico Medio), La Rioja, Argentina. *Ameghiniana* 17: 181–190.

Quiroga, J.C. 1980b. The brain of the mammal-like reptile *Probainognathus jenseni* (Therapsida, Cynodontia). A correlative paleo-neoneurological approach to the neocortex at the reptile-mammal transition. *Journal für Hirnforschung* 21: 299–336.

Quiroga, J.C. 1980c. Descripción de los moldes endocraneanos de dos Cinodontes (Reptilia–Therapsida) de Los Chañares–Triassico medio–de la Provincia de La Rioja (Argentina). Notas sobre al sistema vascular intracraneano y relaciones con los moldes dde otros Cinodontes en función de la morfología de los más antiguos moldes mamalianos conocidos. In *II Congresso Argentino de Paleontología y Bioestratigrafía y I Congreso*

Latinoamericano De Paleontología. Actas, 103–122. Buenos Aires.

Quiroga, J.C. 1984. The endocranial cast of the advanced mammal-like reptile *Therioherpeton cargnini* (Therapsida- Cynodontia) from the Middle Triassic of Brazil. *Journal für Hirnforschung* 25: 285–290.

Radinsky, L. 1968a. A new approach to mammalian cranial analysis, illustrated by examples of prosimian primates. *Journal of Morphology* 124: 167–180.

Radinsky, L. 1968b. Evolution of somatic sensory specialization in otter brains. *Journal of Comparative Neurology* 134: 495–505.

Radinsky, L. 1973a. Are stink badgers skunks? Implications of neuroanatomy for mustelid phylogeny. *Journal of Mammalogy* 54: 585–593.

Radinsky, L. 1973b. Evolution of the canid brain. *Brain, Behavior and Evolution* 7: 169–202.

Radinsky, L. 1976. The brain of Mesonyx, a middle Eocene mesonychid condylarth. *Fieldiana Geology* 33: 323–337.

Radinsky, L. 1977. Brains of early carnivores. *Paleobiology* 3: 333–349.

Radinsky, L. 1981. Brain evolution in extinct South American ungulates. *Brain, Behavior and Evolution* 18: 169–187.

Rodrigues, P.G. 2005. *Endotermia em cinodontes não-mamalianos: a busca por evidências osteológicas.* 133p Dissertação (Mestrado)—Universidade Federal do Rio Grande do Sul, Instituto de Geociências, Porto Alegre, RS. http://www.lume.ufrgs.br/bitstream/handle/10183/6179/000526534.pdf. Accessed 2 Aug 2013.

Rodrigues, P.G., and C.L. Schultz. 2005. The potential use of C.T. scan in the study of the cranial cavities of vertebrate fossils: an example with south american cynodonts In *II Congresso Latino-Americano de Paleontologia de Vertebrados, 2005, Rio de Janeiro. Boletim de Resumos*, 231–231. Rio de Janeiro: Museu Nacional.

Rodrigues, P.G., C.L. Schultz, and M.B. Soares. 2006. A comparative study of the cranial cavities of South American cynodonts from Triassic through CT scan: physiological and evolutionary implications In *XXII Jornadas Argentinas de Paleontología de Vertebrados. Libro de resúmenes*, 32–32. San Juan.

Rodrigues, P.G, Ruf, I., and C.L. Schultz. 2013. Digital reconstruction of the otic region and inner ear of the non-mammalian cynodont *Brasilitherium riograndensis* (Late Triassic, Brazil) and its relevance to the evolution of the mammalian ear. *Journal of Mammalian Evolution*. http://link.springer.com/article/10.1007/s10914-012-9221-2. Accessed 2 Aug 2013 (in press).

Roth, J.J., Roth, E.C., and N. Hotton III. 1986. The parietal foramen eye: their function and fate in therapsidds. In *The Ecology and Biology of Mammal-like Reptiles*, eds. N. Hotton III, P.B. Maclean, J.J. Roth, and E.C. Roth, 173–184. Washington, DC: Smithsonian Institute Press.

Rougier, G.W., and J.R. Wible. 2006. Major changes in the ear region and basicranium of early mammals. In *Amniote Paleobiology: Phylogenetic and Functional Perspectives on the Evolution of Mammals, Birds and Reptiles*, eds. M. Carrano, T.J. Gaudin, R. Blob, and J.R. Wible, 269–311. Chicago: University of Chicago Press.

Rowe, T. 1996. Coevolution of the mammalian middle ear and neocortex. *Science* 273: 651–654.

Rowe, T.B., T.P. Eiting, T.E. Macrini, and R.A. Ketcham. 2005. Organization of the olfactory and respiratory skeleton in the nose of the gray short-tailed opossum *Monodelphis domestica*. *Journal of Mammalian Evolution* 12: 303–336.

Rowe, T.B., T.E. Macrini, and Z.-X. Luo. 2011. Fossil evidence on origin of the mammalian brain. *Science* 332: 955–957.

Ruben, J.A., W.J. Hillenius, N.R. Geist, A. Leitch, T.D. Jones, P.J. Currie, J.R. Horner, and G. Espe III. 1996. The metabolic status of some Late Cretaceous dinosaurs. *Science* 273: 1204–1207.

Ruben, J.A., T.D. Jones, and N.R. Geist. 2003. Respiratory and reproductive paleophysiology of dinosaurs and early birds. *Physiological and Biochemical Zoology* 76(2): 141–164.

Sánchez-Villagra, M.R. 2002. The cerebellar paraflocculus and the subarcuate fossa in *Monodelphis domestica* and other marsupial mammals: ontogeny and phylogeny of a brain-skull interaction. *Acta Theriologica* 47: 1–14.

Silcox, M.T., C.K. Dalmyn, A. Hrenchuk, J.I. Bloch, D.M. Boyer, and P. Houde. 2011. Endocranial morphology of *Labidolemur kayi* (Apatemyidae, Apatotheria) and its relevance to the study of brain evolution in Euarchontoglires. *Journal of Vertebrate Paleontology* 31: 1314–1325.

Simpson, G.G. 1927. Mesozoic Mammalia. IX. The brain of Jurassic mammals. *American Journal of Science* 214: 259–268.

Simpson, G.G. 1937. Skull structure of the Multituberculata. *Bulletin of the American Museum of Natural History* 73: 727–763.

Starck, D. 1979. *Vergleichende Anatomie der Wirbeltiere auf evolutionsbiologischer Grundlage, Bd. 2, XII.* Berlin: Springer.

Striedter, G.F. 2005. *Principles of Brain Evolution*. Massachusetts: Sinauer Associates, Sunderland.

Ulinski, P.S. 1986. Neurobiology of the therapsid-mammal transition. In *The Ecology and Biology of Mammal-like Reptiles*, ed. N. Hotton III, P.B. Maclean, J.J. Roth, and E.C. Roth, 149–171. Washington, DC: Smithsonian Institution Press.

Watson, D.M.S. 1913. Further notes on the skull, brain, and organs of special sense of *Diademodon*. *The Annals and Magazine of Natural History, Series* 8(12): 217–228.

Wible, J.R., and G.W. Rougier. 2000. Cranial anatomy of *Kryptobaatar dashzevegi* (Mammalia, Multituberculata), and its bearing on the evolution of mammalian characters. *Bulletin of the American Museum of Natural History* 247: 1–120.

Zerfass, H., E.L. Lavina, C.L. Schultz, A.J.V. Garcia, U.F. Faccini, and F. Chemale Jr. 2003. Sequence-stratigraphy of continental strata of Southernmost Brazil: a contribution to Southwestern Gondwana palaeogeography and palaeoclimate. *Sedimentary Geology* 161: 85–105.